KeAi
CHINESE ROOTS
GLOBAL IMPACT

Contents lists available at ScienceDirect

Petroleum Science

journal homepage: www.keaipublishing.com/en/journals/petroleum-science



Original Paper

Coupling analysis of transient cuttings transport and tubular mechanical behaviors in extended-reach drilling



Jun Zhao a, b, Wen-Jun Huang a, b, *, De-Li Gao a, b, **, Wen-Long Li c

- ^a MOE Key Laboratory of Petroleum Engineering, China University of Petroleum (Beijing), Beijing, 102249, China
- b National Key Laboratory of Petroleum Resources and Engineering, China University of Petroleum (Beijing), Beijing, 102249, China
- ^c Tianjin Branch of CNOOC Ltd., Tianjin, 300459, China

ARTICLE INFO

Article history: Received 7 August 2024 Received in revised form 10 January 2025 Accepted 12 January 2025 Available online 13 January 2025

Edited by Jia-Jia Fei

Keywords: Extended-reach drilling Hole cleaning Transient cuttings transport Theoretical modeling Drilling optimization

ABSTRACT

It is generally believed that cuttings have a significant impact on the forces of tubular string in extendedreach drilling. However, there are few studies attempted to investigate and quantify it. In this paper, a three-layer transient model for cuttings transport is established to simulate the characteristics of dynamic cuttings transport over time under various conditions. The simulation results indicate that the change in drilling parameters like ROP (rate of penetration) and flow rate of drilling fluid will lead to the non-uniform distribution of cuttings bed. And the alternation of drilling and circulation will lead to a clear wavy distribution of cuttings bed in the wellbore. Then, the effect of cuttings on tubular string is obtained through a large number of numerical simulations and the nonlinear regression method, and this influence is introduced into the conventional stiff rod model of tubular string. Finally, the transient model for cuttings transport is coupled with the modified tubular mechanic model and applies to a case study of extended-reach drilling. The results show that there is a delay effect for the effect of the changes in drilling parameters on the ground torques because the changes in drilling parameters occur instantaneously, while the changes in cuttings bed distribution are slow due to its low transport velocity. Based on the coupling analysis of transient cuttings transport and tubular mechanical behaviors, the drilling parameters are optimized, including the recommended adjustment period and adjustment range for the ROP, the proper drilling time for the increased flow rate. Furthermore, the circulation and back reaming are optimized. For circulation, the keys are choosing appropriate time interval between the two adjacent circulations and the time for each circulation. To avoid pipe stuck, at least 20 min of circulation is required to remove the cuttings bed near the large-sized BHA ((Bottom Hole Assembly)) before back reaming, and the maximum back reaming velocity should be smaller than the minimum transport velocity of the uniform bed.

© 2025 The Authors. Publishing services by Elsevier B.V. on behalf of KeAi Communications Co. Ltd. This is an open access article under the CC BY-NC-ND license (http://creativecommons.org/licenses/by-nc-nd/4.0/).

1. Introduction

Extended-reach drilling technology enables the effective development of oil and gas resources in challenging environments, including offshore and mountainous regions, by overcoming surface condition limitations. (Huang and Gao, 2021). With the development of drilling technologies, the economic benefits of extended-reach wells are constantly improving, now their

E-mail addresses: huangwenjun1986@126.com (W.-J. Huang), gaodeli_team@ 126.com (D.-L. Gao).

production can reach 4—8 times that of vertical wells (Li, 2018). Multiple extended-reach wells can be drilled on one drilling platform (Zhao et al., 2024). This not only increases the control area of a single platform, but also reduces the cost of moving drilling platforms at sea and significantly saves ground costs on land. Therefore, the application of extended-reach wells is becoming increasingly widespread.

However, poor hole cleaning and high drag & torque are challenges that has always been faced in extended-reach drilling. As the highly inclined section become longer, the increasing friction usually leads to insufficient WOB (weight on bit). In the unclean wellbore, the additional resistance of cuttings on tubular string makes this problem more prominent, which may result in frequent

^{*} Corresponding author.

^{**} Corresponding author.

backpressure and even stuck (Zhu et al., 2022). To alleviate these two issues, numerous studies have been conducted from different aspects, including analysis of tubular mechanical behaviors and prediction of hole cleaning in wellbore.

For tubular mechanics issue, the related analyses are usually carried out based on soft rope model (Johancsik et al., 1984) and stiff rod model (Ho. 1988: Mitchell and Samuel, 2009), Huang et al. (2018, 2019) discussed the buckling behaviors and critical buckling load of tubular string. Through experiments, Zhang et al. (2019) obtained the relationship between the torque and cuttings bed height, Song et al. (2019) proposed an empirical formula to calculate the friction factor under different cuttings bed height in microhole-horizontal-well. Huang and Gao (2021) introduced the mechanical resistance at the connectors, and further analyzed the pipe stuck mechanism of open-hole keyway in extended-reach drilling. Zhao et al. (2022a) believed that the local accumulation of cuttings near the connectors is one of the main reasons for pipe stuck. Zhao et al. (2022b) believed that the curvature discontinuity of well trajectory and stiffness discontinuity at the connection of two tubular string with different sizes has a non-negligible impact on pipe load. Mahjoub et al. (2023) discussed the drag & torque on tubular string when the drilling fluid circulates or not. Dao et al. (2023) established a theoretical model for tubular string to consider the influence of the number and locations of bow-spring centralizers on tubular mechanical behaviors. Zhu et al. (2024) analyzed the effect of cuttings on the friction behaviors between the Fe bulk and diamond-like carbon film from a qualitative perspective.

On the whole, the calculation accuracy of the soft rope model in curved well sections is relatively low. Although stiff rod model compensates for this drawback, both soft rope model and stiff rod model usually assume that the wellbore is in ideal cleaning, neglecting the influence of cuttings bed. At present, there has no reliable prediction model of drag & torque considering the effects of cuttings resistance.

For hole cleaning issue, the current cuttings transport models include steady models (Gavignet and Sobey, 1989; Nguyen and Rahman, 1998) and transient models (Martins et al., 1999; Naganawa and Nomura, 2006; Guo et al., 2010). The steady models focus on the characteristics of cuttings transport on a certain annular cross-section (Zhao et al., 2024), while the transient models can analyze the variation of relevant parameters over time in the entire wellbore (Zhu, 2022). Therefore, transient models for cuttings transport have more advantages than steady models.

The theoretical modeling works of the transient models began with Martins et al. (1999) and Doan et al. (2003), and was refined by Naganawa and Nomura (2006). Martins et al. (1999) and Doan et al. (2003) derived the governing equations for the two-layer transient models by applying the basic principles of fluid mechanics, i.e., mass conservation and momentum conservation to each layer. However, they ignored the difference in flow velocity between cuttings and fluid in the suspended layer. Naganawa and Nomura (2006) compensated for this deficiency and introduced the mass exchange effect between cuttings bed and suspended layer. Guo et al. (2010) first established a three-layer transient model for cuttings transport and provided a detailed introduction to numerical solution methods.

On the basis of Naganawa and Nomura (2006) and Guo et al. (2010), many improvement work had been conducted. Naganawa et al. (2017) combined the transient model with measured ECD (equivalent circulating density) to reveal abnormal downhole conditions. Zhang et al. (2018) discussed the conversion of cuttings flow patterns during the dynamic cuttings transport process. Zhang et al. (2020) combined the three-layer transient model for cuttings transport with CFD method, providing a more detailed description

of the dynamic cuttings transport characteristics. Zhu et al. (2021) made two important revisions to the transient model: one is presenting the correction coefficients of gravitational acceleration considering the effect of buoyancy, the other is improving the quantitative calculation method of mass exchange effect through the diffusion equation of cuttings. Zhu et al. (2022) proposed the modified transient model under the pump shutdown operation and analyzed the risk of pipe stuck in build-up section due to the slippage of cuttings. Miao et al. (2023) predicted the ECD in extended-reach drilling with the transient model.

Overall, it is generally believed that there is a coupling effect between cuttings transport and tubular mechanical behaviors, but there are few studies attempted to investigate this complicated interaction problem (Zhao et al., 2024). In extended-reach drilling, the existence of cuttings beds is inevitable, and the coupling effect between cuttings and tubular string is quite prominent in such a long and narrow wellbore. Moreover, the hole cleaning varies with time, drilling parameters and operations. Therefore, it is difficult to accurately analyze this coupling effect through conventional steady models.

In this paper, a three-layer transient model for cuttings transport is established to simulate the characteristics of dynamic cuttings transport over time under various conditions, including the change in drilling parameters like *ROP* and flow rate of drilling fluid, as well as different operations like drilling, circulation and back reaming. Then, this transient model is coupled with the modified tubular mechanic model, in which the effect of cuttings on tubular string is obtained through a large number of numerical simulations and the nonlinear regression method. Finally, a case study of extended-reach drilling is carried out to demonstrate the importance of coupling transient cuttings transport with tubular mechanical behaviors and its beneficial effects.

2. Transient model for cuttings transport

2.1. Model development

The three-layer flow of cuttings transport consists of three parts: the upper suspended layer, the middle moving bed, and the lower uniform bed. The suspended layer is the main area for fluid flow, and the moving bed and uniform bed are dense packed layers of cuttings. In suspended layer, cuttings are in suspension with relatively high transport velocity. In moving bed, cuttings are mainly transported in the form of rolling. In uniform bed, cuttings are mainly transported in the form of sliding. If the driving force on the uniform bed is insufficient, the uniform bed will convert into a stationary bed that is difficult to clean up.

The schematic diagram of the transient three-layer modeling is shown in Fig. 1. At first, the following assumptions are introduced to simplify the extremely complex problem of real cuttings transport: (1) The flow in the annulus is time-dependent and 1D (axial direction of the annulus). (2) All physical properties and variables are represented by the average characteristics of each layer. (3) The slip between drilling fluid and cuttings is only considered in suspended layer. (4) Drilling fluid and cuttings are incompressible, and the rheological properties of the solid-liquid system is the same as the drilling fluid. (5) The size, physical properties and spherical of cuttings are the same. (6) The cuttings concentration in uniform/stationary bed is 0.52, the cuttings concentration in moving bed is 88% of that in uniform/stationary bed (Guo et al., 2010). The distribution of cuttings in the suspended layer accords with the diffusion law.

For the cuttings and fluid in the suspended layer, moving bed and uniform bed, the continuity equations are as follows:

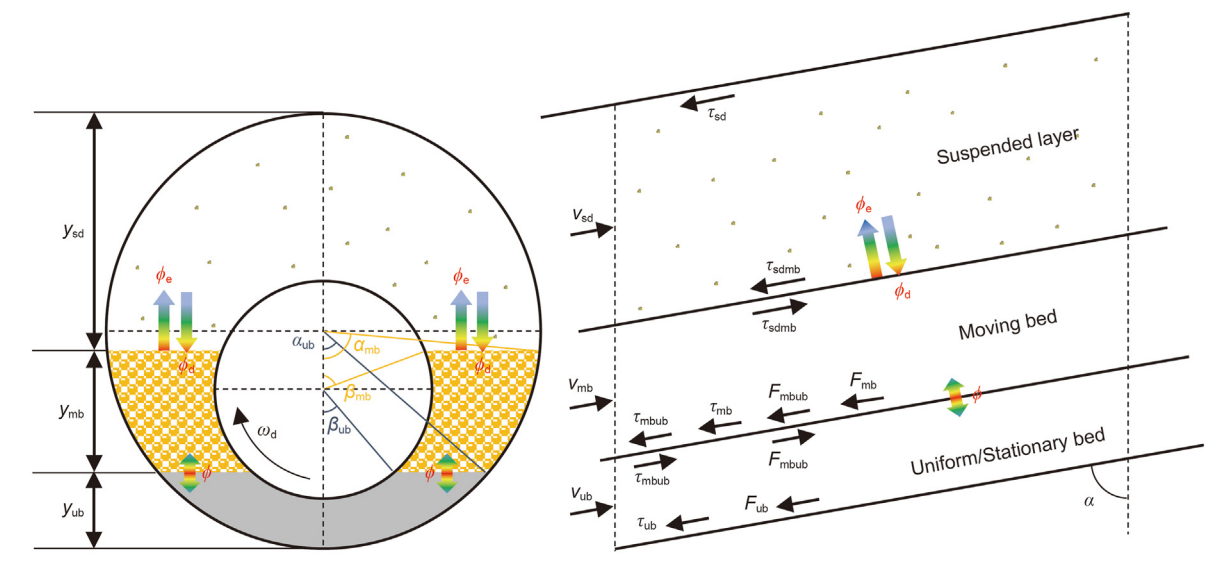


Fig. 1. Schematic diagram of three-layer modeling.

$$\frac{\partial \left(\rho_{\text{sd,f}}C_{\text{sd,f}}A_{\text{sd}}\right)}{\partial t} + \frac{\partial \left(\rho_{\text{sd,f}}C_{\text{sd,f}}v_{\text{sd,f}}A_{\text{sd}}\right)}{\partial x} = \phi_{\text{sd,f}}$$
(1)

$$\frac{\partial \left(\rho_{sd,c}C_{sd,c}A_{sd}\right)}{\partial t} + \frac{\partial \left(\rho_{sd,c}C_{sd,c}V_{sd,c}A_{sd}\right)}{\partial x} = \phi_{sd,c} \tag{2}$$

$$\frac{\partial v_{\text{sd,c}}}{\partial t} + v_{\text{sd,c}} \frac{\partial v_{\text{sd,c}}}{\partial x} = -g_{\text{sd,c}} \cos \alpha - \frac{1}{\rho_c} \frac{\partial p}{\partial x} - \frac{\tau_{\text{sd,c}} s_{\text{sd}}}{\rho_c A_{\text{sd}}} - \frac{\tau_{\text{sdmb}} s_{\text{sdmb}}}{\rho_c A_{\text{sd}}} + \frac{F_{\text{D}}}{\rho_c C_{\text{sd,c}} A_{\text{sd}}} + \frac{v_{\text{sd,c}} \phi_{\text{sd,c}}}{\rho_c C_{\text{sd,c}} A_{\text{sd}}} \tag{6}$$

$$\frac{\partial \nu_{mb}}{\partial t} + \nu_{mb} \frac{\partial \nu_{mb}}{\partial x} = -g_{mb} \cos \alpha - \frac{1}{\rho_{mb}} \frac{\partial p}{\partial x} - \frac{\tau_{mb} s_{mb}}{\rho_{mb} A_{mb}} - \frac{\tau_{mbub} s_{mbub}}{\rho_{mb} A_{mb}} + \frac{\tau_{sdmb} s_{sdmb}}{\rho_{mb} A_{mb}} - \frac{\tau_{mbub} s_{mbub}}{\rho_{mb} A_{mb}} - \frac{\tau_{mb} s_{mbub}}{\rho_{mb} A_{mb}} - \frac{\tau_{mb} s_{mb}}{\rho_{mb} A_{mb}} - \frac{\tau_{mb} s_{mb}}{\rho_$$

$$\frac{\partial(\rho_{\rm mb}A_{\rm mb})}{\partial t} + \frac{\partial(\rho_{\rm mb}\nu_{\rm mb}A_{\rm mb})}{\partial x} = -\phi_{\rm sdmb} + \phi_{\rm mbub} \tag{3}$$

$$\frac{\partial(\rho_{\rm ub}A_{\rm ub})}{\partial t} + \frac{\partial(\rho_{\rm ub}\nu_{\rm ub}A_{\rm ub})}{\partial x} = -\phi_{\rm mbub} \tag{4}$$

where A is cross-sectional area, m^2 ; C is cuttings concentration, dimensionless; v is velocity, m/s; ρ is density, kg/m^3 ; ϕ is mass flux, $kg/(s \cdot m)$. The subscript c represents cuttings, f represents fluid, mb represents the moving bed, mbub represents the interface between the moving bed and uniform bed, sd represents the suspended layer, ub represents the uniform bed.

According to the mechanical analysis of the transient threelayer model, the momentum equations can be expressed as:

$$\begin{split} &\frac{\partial \nu_{sd,f}}{\partial t} + \nu_{sd,f} \frac{\partial \nu_{sd,f}}{\partial x} = -g_{sd,f} \cos \alpha - \frac{1}{\rho_f} \frac{\partial p}{\partial x} - \frac{\tau_{sd,f} s_{sd}}{\rho_f A_{sd}} - \frac{\tau_{sdmb} s_{sdmb}}{\rho_f A_{sd}} \\ &\frac{F_D}{\rho_f C_{sd,f} A_{sd}} + \frac{\nu_{sd,f} \phi_{sd,f}}{\rho_f C_{sd,f} A_{sd}} \end{split}$$

$$\begin{split} \frac{\partial \nu_{ub}}{\partial t} + \nu_{ub} \frac{\partial \nu_{ub}}{\partial x} &= -g_{ub} \cos \alpha - \frac{1}{\rho_{ub}} \frac{\partial p}{\partial x} - \frac{\tau_{ub} s_{ub}}{\rho_{ub} A_{ub}} + \frac{\tau_{mbub} s_{mbub}}{\rho_{ub} A_{ub}} \\ &+ \frac{F_{mbub} - F_{ub}}{\rho_{ub} A_{ub}} - \frac{\nu_{ub} \phi_{mbub}}{\rho_{ub} A_{ub}} \end{split} \tag{8}$$

where F is dry friction force, N; F_D is the drag force between the cuttings and fluid in the suspended layer, N; g is the gravitational acceleration, m/s²; α is the inclination, °; $\frac{\partial p}{\partial x}$ is the pressure gradient, Pa/m; τ is shear stress, Pa. The subscript sdmb represents the interface between the suspended layer and moving bed.

In the uniform bed, the cuttings are mainly transported in the form of sliding, this requires that the driving force of the uniform bed must be greater than the resistance, namely:

$$A_{\rm mb}\frac{\Delta p}{\Delta L} + F_{\rm mbub} + \tau_{\rm mbub} s_{\rm mbub} \ge \rho_{\rm ub} A_{\rm ub} g_{\rm ub} \cos \alpha + F_{\rm ub} \tag{9}$$

Once Eq. (9) does not hold, it means that the uniform bed cannot continue to move upwards and converts into a stationary bed. In this case, the continuity equations and momentum equations of the

(5)

cuttings and fluid in the suspended layer, as well as moving bed remain unchanged, but the continuity equations of uniform bed is updated to the continuity equations of stationary bed:

$$\frac{\partial(\rho_{\rm sb}A_{\rm sb})}{\partial t} = -\phi_{\rm mbsb} \tag{10}$$

where the subscript mbsb represents the interface between the moving bed and stationary bed, sb represents the stationary bed.

2.2. Mass exchange effect

In the process of cuttings transport, due to the effects of cuttings gravity and turbulent diffusion, the suspended cuttings will deposit while the sedimentary cuttings will be resuspended, which cause the change in cuttings quality in the longitudinal direction, as shown in Fig. 2.

Naganawa and Nomura (2006), Guo et al. (2010) and Tong et al. (2021) used two critical velocities to calculate the mass exchange flux. For the deposition mass flux, the key is to obtain the cuttings deposition velocity (Ramadan et al., 2005) in the suspended layer, and they are calculated by:

$$\begin{cases} \phi_{\text{sd,f}} = C_{\text{sd,f}} \rho_{\text{f}} s_{\text{sdmb}} v_{\text{dep}} \frac{C_{\text{sd,c}}}{C_{\text{mb}}} \\ \phi_{\text{sd,c}} = C_{\text{sd,c}} \rho_{\text{c}} s_{\text{sdmb}} v_{\text{dep}} \frac{C_{\text{sd,c}}}{C_{\text{mb}}} \end{cases}$$

$$(11)$$

$$v_{\rm dep} = \left(1 - C_{\rm sd,c}\right)^{m_{\rm dep}} \cdot \sqrt{\frac{4d_{\rm c}g\left(\rho_{\rm c} - \rho_{\rm f}\right)\sin\alpha}{3\rho_{\rm f}C_{\rm D}}} \tag{12}$$

where C_D is the drag coefficient; $m_{\rm dep}$ is the deposition coefficient; $v_{\rm dep}$ is the cuttings deposition velocity, m/s.

For the entrainment mass flux, the key is to obtain the critical resuspension velocity of cuttings (*CRV*, *Oroskar and Turian*, 1980), and they are calculated by:

$$\begin{cases} \phi_{e,f} = (1 - C_{mb})\rho_f s_{sdmb} \nu_{ent} \\ \phi_{e,c} = C_{mb}\rho_c s_{sdmb} \nu_{ent} \end{cases}$$
 (13)

$$v_{\text{ent}} = \begin{cases} m_{\text{ent}} \sin \alpha \left(v_{\text{sd,f}} - CRV \right) & \text{if } v_{\text{sd,f}} > CRV \\ 0 & \text{if } v_{\text{sd,f}} \le CRV \end{cases}$$
 (14)

where m_{dep} is the entrainment coefficient; v_{ent} is the critical resuspension velocity of cuttings, m/s.

According to Eq. (14), the entrainment velocity is closely related

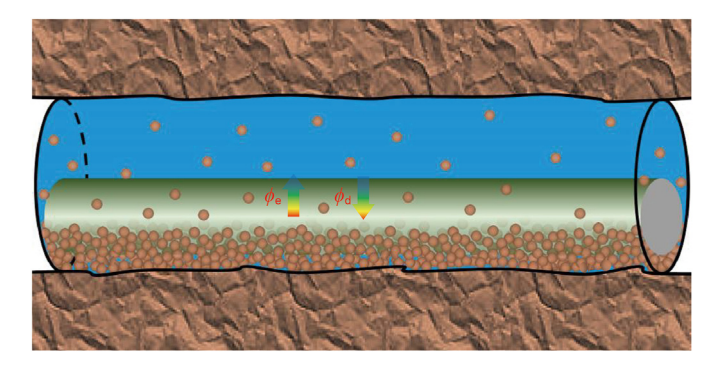


Fig. 2. Mass exchange between the cuttings bed and suspended layer.

to the fluid velocity in suspended layer. When the fluid velocity is less than the critical resuspension velocity of cuttings, the entrainment velocity is 0 m/s, which means the entrainment mass flux is also 0 kg/(s·m). However, Hirpa and Kuru (2020) has demonstrated through experiments that turbulent diffusion still exists even at very low fluid velocity, i.e., the above method has obvious shortcomings.

Therefore, Zhu et al. (2021) presented a new method for calculating mass exchange flux between the suspended layer and cuttings bed by combining the cuttings diffusion equation. Assuming that the cuttings deposition velocity is independent of position, the diffusion equation for cuttings in an inclined annulus is expressed as:

$$\varepsilon_{c} \frac{\partial^{2} C}{\partial v^{2}} + v_{dep} \frac{\partial C}{\partial v} = 0$$
 (15)

where ε_c is the mean diffusion coefficient of cuttings (Walton, 1995; Wang, 2008), m²/s.

In extended-reach drilling, the effect of pipe rotation on cuttings transport cannot be neglected. Zhao et al. (2024) introduced a stirring diffusion factor to modify the mean diffusion coefficient of cuttings, and further characterize the influence of pipe rotation on cuttings transport. Then, the amended diffusion equation is:

$$(1 + \lambda_{\varepsilon_c})\varepsilon_c \frac{\partial^2 C}{\partial v^2} + \nu_{\text{dep}} \frac{\partial C}{\partial v} = 0$$
 (16)

$$\begin{split} &\lambda_{\varepsilon_{c}} = (0.467022 - 0.948927e) \cdot \left[0.170859 - \frac{0.00095 \rho_{f} v_{r} d_{o} (d_{w} - d_{o}) v_{f}}{\mu_{e}} \right] \cdot \\ &\left(0.002369 + \frac{47.274771ROP}{v_{f}} \right) \cdot \left[593.082688 - \frac{0.091051 \rho_{f} v_{f} (d_{w} - d_{o})}{\mu_{e}} \right] \cdot \\ &\left(\frac{d_{o}}{d_{w}} \right)^{4.860738} \cdot \left[0.297038 - \frac{0.985878 v_{f}^{2}}{g (d_{w} - d_{o})} + 1.033993 \frac{v_{f}^{4}}{g^{2} (d_{w} - d_{o})^{2}} \right] \end{split}$$

where d_0 is the outer diameter of drill string, m; d_w is the wellbore diameter, m; e is pipe eccentricity; ROP is rate of penetration, m/h; v_r is the rotational velocity of outer wall of drill string, m/s; λ_{ε_c} is the stirring diffusion factor; μ_e is the effective viscosity of the fluid, Pa·s.

The boundary condition of Eq. (16) is $C=C_{mb}$ at the interface of moving bed and suspended layer, so the solution of Eq. (16) is:

$$C(y) = C_{\text{mb}} \exp \left[-\frac{\nu_{\text{dep}} \sin \alpha}{(1 + \lambda_{\varepsilon_c})\varepsilon_c} (y - y_{\text{mb}} - y_{\text{ub}}) \right]$$
 (18)

By integrating Eq. (18) within the suspended layer, the mean cuttings concentration in suspended layer can be obtained as (Zhu, 2022):

$$C_{\text{sd,c}} = C_{\text{mb}}(I_{\text{O}} - I_{\text{I}}) / A_{\text{sd}} \tag{19}$$

$$\begin{split} I_{O} &= \int_{a1}^{a2} \exp \left[-\frac{\nu_{dep}}{(1 + \lambda_{\varepsilon_{c}})\varepsilon_{c}} \left(\frac{d_{o}}{2} + \frac{d_{o}}{2} \sin \theta - y_{mb} - y_{ub} \right) \right] \\ &= \frac{d_{o}^{2} \cos^{2} \theta}{2} d\theta \end{split} \tag{20}$$

$$I_{I} = \int_{a3}^{a4} \exp\left[-\frac{v_{\text{dep}}}{(1+\lambda_{\varepsilon_{c}})\varepsilon_{c}} \left(\frac{d_{o}}{2} + \frac{d_{i}}{2}\sin\gamma - y_{\text{mb}} - y_{\text{ub}} - E\right) \right]$$

$$\times \left[\frac{d_{i}^{2}\cos^{2}\gamma}{2}d\gamma\right]$$
(21)

where d_i is the inner diameter of drill string, m; E is the eccentric distance, m; y is bed height, m.

Thus, the variation of cuttings concentration in the suspended layer per unit time is calculated by:

$$\Delta C_{\rm sd,c} = \left(C_{\rm sd,c}^{n+1} - C_{\rm sd,c}^{n} \right) / \Delta t \tag{22}$$

where $\Delta C_{\rm sd,c}$ is the variation of cuttings concentration, s^{-1} ; Δt is the time step, s.

The mass exchange flux can be expressed as:

$$\phi_{\text{sd,c}} = \Delta C_{\text{sd,c}} \rho_{\text{c}} A_{\text{sd}} \tag{23}$$

$$\phi_{\text{sd.f}} = \Delta C_{\text{sd.c}} \rho_f A_{\text{sd}} (1 - C_{\text{mb}}) / C_{\text{mb}}$$
(24)

$$\phi_{\text{sdmb}} = \Delta C_{\text{sd,c}} \rho_{\text{mb}} A_{\text{sd}} / C_{\text{mb}} \tag{25}$$

In addition, the mass exchange flux between the moving bed and uniform/stationary bed is calculated by (Guo et al., 2010):

$$\phi_{\text{mbub}} = \rho_{\text{mb}} (y_{\text{mb}} s_{\text{mbub}} - A_{\text{mb}}) / C_{\text{mb}}$$
 (26)

3. Numerical solution for the transient model

3.1. Numerical solution method

Due to the strong nonlinear of the governing equations and complicated coupling relationship between the involved parameters, the stability-enhancing two-step (SETS) method based on semi-implicit techniques (Mahaffy, 1982) is adopted to solve the transient model. Its main advantage is that larger time step sizes are permitted while ensuring the stability of numerical solutions, thereby reducing computational costs.

Firstly, the staggered mesh and first-order upwind differencing scheme are applied for the discretization of differential equations. On staggered mesh, scalar variables, including cross-sectional area A, concentration C and pressure p are stored in the grid center (red dashed line), while vectors variables, including velocities are stored in the grid interface (black solid line), as shown in Fig. 3.

Secondly, two important treatments are made in SETS method

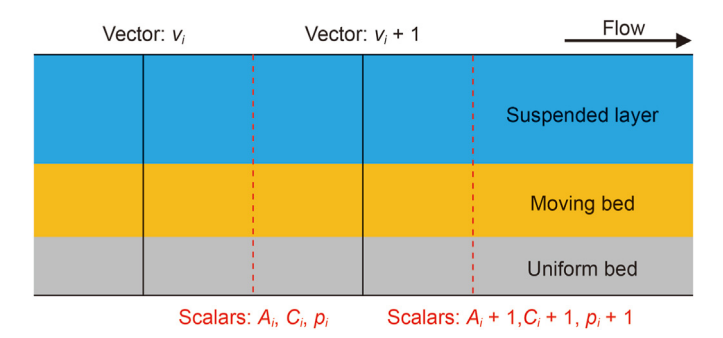


Fig. 3. Schematic diagram of staggered grid.

to improve the stability of numerical calculations. One is the convection term in Eqs. (5)–(8):

$$v_{j+1/2}\nabla_{j+1/2}v = \begin{cases} \frac{v_{j+1/2}\left(v_{j+1/2} - v_{j-1/2}\right)}{\Delta x_{j+1/2}} & v_{j+1/2} \ge 0\\ \frac{v_{j+1/2}\left(v_{j+3/2} - v_{j+1/2}\right)}{\Delta x_{j+1/2}} & v_{j+1/2} < 0 \end{cases}$$
(27)

where $\Delta x_{j+1/2} = 0.5 (\Delta x_j + \Delta x_{j+1})$.

The other is that shear stress can be calculated as:

$$\tau^{n} = \frac{1}{2} f \rho |v^{n}| \left(2v^{n+1} - v^{n} \right) = f \rho |v^{n}| v^{n+1} - \tau^{n}$$
 (28)

where f is friction factor.

Then, please refer Guo et al. (2010) and Zhu (2022) for the detailed discretized equations and solution steps.

3.2. Model validation

The transient model validated through the previous experiments (Kim et al., 2014; Zhang et al., 2020), as shown in Fig. 4. Compared with the Kim's experiments, the average predicted error of cuttings concentration is 4.26% when the supplied cuttings concentration is 4%, and 5.18% when the supplied cuttings concentration is 8%, as shown in Fig. 4(a). Compared with the Zhang's experiments (Zhang et al., 2020), the average predicted error of cuttings bed height is 12.60%, as shown in Fig. 4(b). Overall, the results indicate good performance of the transient model in predicting the cuttings transport.

4. Coupling of the transient model for cuttings transport and tubular mechanical behaviors

It is generally considered that cuttings have a significant impact on forces of tubular string. Zhang's experiments (Zhang et al., 2019) show that the accumulation of cuttings in the wellbore leads to significant increase in the torque on drill string. Zhao et al. (2022a) believed that the axial motion of drill string may results in local high cuttings bed at connectors in horizontal hole section, which is one of the main reasons for pipe sticking. Zhu et al. (2022) simulated the cuttings transport characteristics when the pump is stopped. The results show that cuttings will slip down at an inclination of $40^{\circ}-60^{\circ}$ and form heavily stacking, causing potential risk of pipe sticking.

Therefore, an improved drag & torque model for tubular string is presented considering the effect of cuttings. As shown in Fig. 5, a contact force $N_{\text{t-w}}$ will be generated due to the contact between the connector and wellbore. Meanwhile, the cuttings in the wellbore will exert a contact force $N_{\text{t-c}}$ on tubular string due to the collision and relative motion between cuttings and tubular string. The total contact force of tubular string can be expressed as:

$$N_{t} = N_{t-w} + N_{t-c} \tag{29}$$

where N is the total contact force per unit length, N/m. The subscript t represents the tubular string, w represents the wellbore.

During the drilling process, tens of thousands of cuttings particles are generated every second due to rock breaking. Thus, it is nearly impossible to directly obtain $N_{\text{t-c}}$ based on mechanical analysis. According to the authors' previous study (Zhao et al., 2024), a pipe-cuttings contact stress uniformly distributed on the outer wall of tubular string is used to equivalently represent the

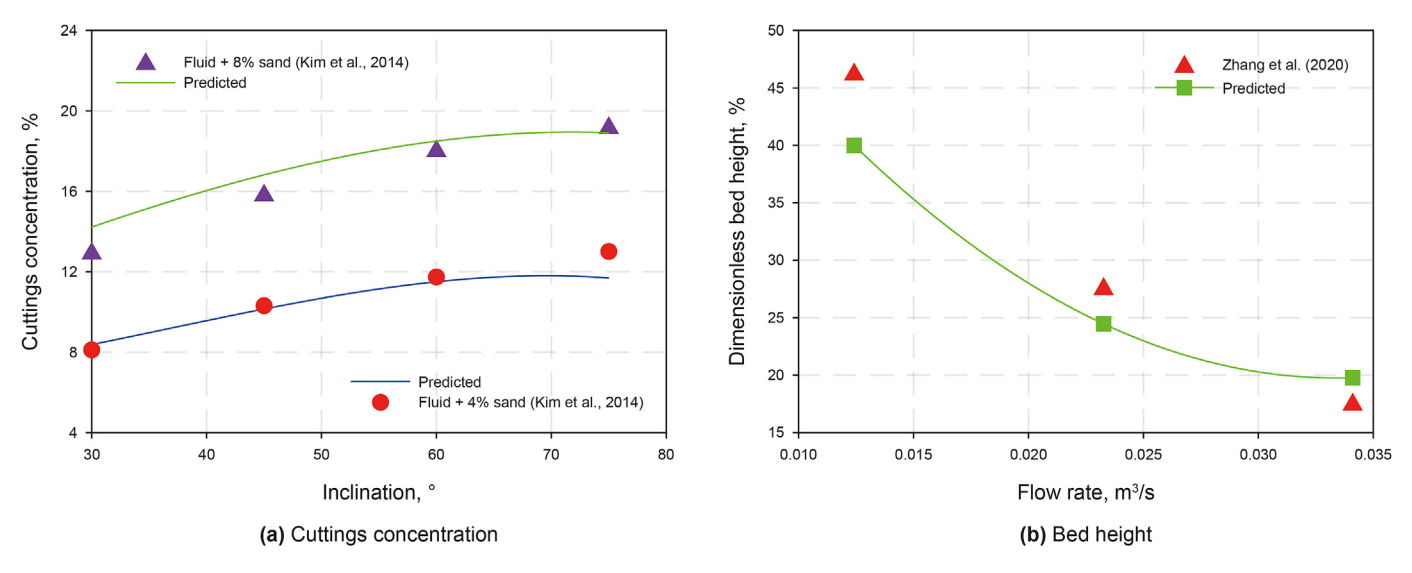


Fig. 4. Validation of the transient model.

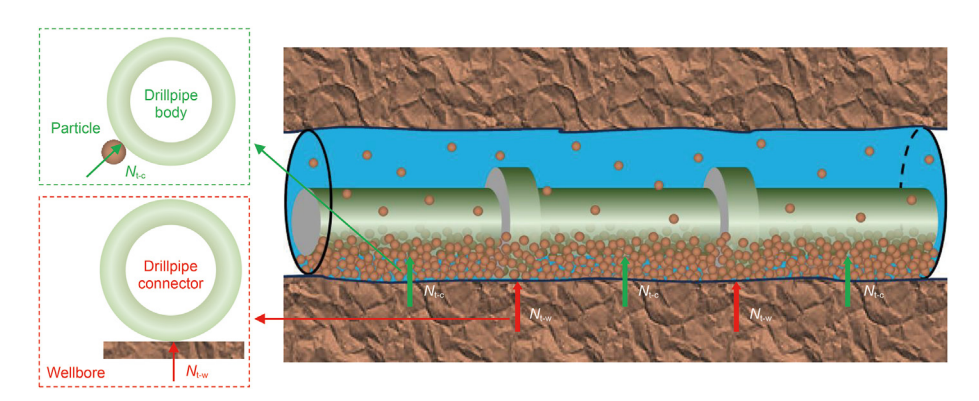


Fig. 5. Schematic diagram of contact forces.

cumulative effect of cuttings on pipe load. It is calculated by:

$$\sigma_{\rm n} = \frac{\sum_{i=1}^{n} \int_{i} F_{\rm n,i} dt}{A_{\rm T} \Delta t}$$
 (30)

where A_T is the area of the outer wall of tubular string, m^2 ; $F_{n,i}$ is the contact force of particle i on tubular string, N; Δt is the time, s; σ_n is the pipe-cuttings contact stress, Pa.

Through 440 sets of numerical simulations and the nonlinear regression method, Zhao et al. (2024) established the calculation formula of pipe-cuttings contact stress. On this basis, the range of parameters was expanded and 120 sets of numerical simulation results were added, the improved calculation formula of pipe-cuttings contact stress is:

where H is the dimensionless cuttings bed height; q is the gravity per unit length of tubular string, N/m.

Then, the contact force result from cuttings is calculated by:

$$N_{t-c} = \sigma_n \cdot \pi d_o \tag{32}$$

For the improved drag & torque model for tubular string, the assumptions are as follows: (1) The axis of the tubular string coincides with the axis of the wellbore; (2) Stress and deformation of the tubular string are elastic; (3) The effects of vibration damping and dynamic effects are neglected. The transfer of axial force and torque on tubular string gives:

$$\sigma_{n} = \frac{2.906037 \times 10^{-6} q}{\pi d_{o}} (1 - e)^{-0.663737} \cdot \left[\frac{\rho_{f} v_{r} d_{o} (d_{w} - d_{o}) v_{f}}{\mu_{e}} \right]^{-0.110205} \cdot \left(\frac{ROP}{v_{f}} \right)^{-0.128743} \cdot \left(\frac{d_{o}}{d_{w}} \right)^{-14.695113} \cdot \left[\frac{\rho_{f} v_{f} (d_{w} - d_{o})}{\mu_{e}} \right]^{0.420274} \cdot \left[\frac{v_{f}^{2}}{g (d_{w} - d_{o})} \right]^{-0.049423} \cdot H^{3.065939}$$
(31)

J. Zhao, W.-J. Huang, D.-L. Gao et al. Petroleum Science 22 (2025) 1252—1269

$$\begin{cases} \frac{dF_e}{ds} + EIk\frac{dk}{ds} + w_{bp}\cos\alpha - \mu_d N_t \left(1 - \frac{1}{2}kd_0\cos\theta\right) = 0\\ \frac{dM_t}{ds} - \frac{1}{2}d_0\mu_t N_t = 0 \end{cases}$$
(33)

where E is Young's modulus of tubular string, N/m^2 ; F_e is the axial force, N; I is the moment of inertia of tubular string, m^4 ; k is the trajectory curvature, m^{-1} ; M_t is the torque, $N \cdot m$; w_{bp} is the buoyant weight per meter of tubular string, N/m; θ is the contact angle between the tubular string and wellbore, °. μ_d and μ_t are the axial and circumferential friction factor, respectively (Zhao et al., 2024).

In the drilling process, the drilling parameters will be continuously adjusted with the increase of well depth to accommodate the drilling requirements and changing downhole conditions. So the first step is to determine the distribution of cuttings bed in the entire wellbore with the different drilling parameters based on the transient model. Then, the results of predicted cuttings bed are taken as the inputs for the drag & torque model, and the contact force N_{t-c} at each discrete point is obtained by Eqs. (31) and (32). Combining with the finite difference method, the axial force and torque along the tubular string can be solved through Eq. (33).

5. Case study

In this paper, the developed models are applied to the extended-reach well X to analyze the coupling effect between the tubular mechanical behaviors and dynamic cuttings transport. The well profile and well structure of X are shown in Fig. 6.

Overall, poor hole cleaning in drilling $12^1/_4$ -in. Section is quite serious, resulting in frequent pipe stuck and additional time cost. It is originally planned to drill to 4205 m, but when dilled to 3706 m, there encouraged severe problem of WOB transfer and impassable tight spot while back reaming. Considering the drilling risk, the $12^1/_4$ -in. Section is completed at 3716 m. By comparison, the $9^1/_4$ -in. Section is well cleaned during drilling because of high fluid return velocity, and is completed through "one trip". Therefore, the $12^1/_4$ -in. Section is the main object of case study in the following content, and basic parameters for calculation are given in Table 1 in which the pipe eccentricity $e_{\rm max}$ is calculated by:

$$e_{\text{max}} = \frac{d_{\text{w}} - d_{\text{con}}}{d_{\text{w}} - d_{\text{o}}} \tag{34}$$

where d_{con} is the outer diameter of connector, m.

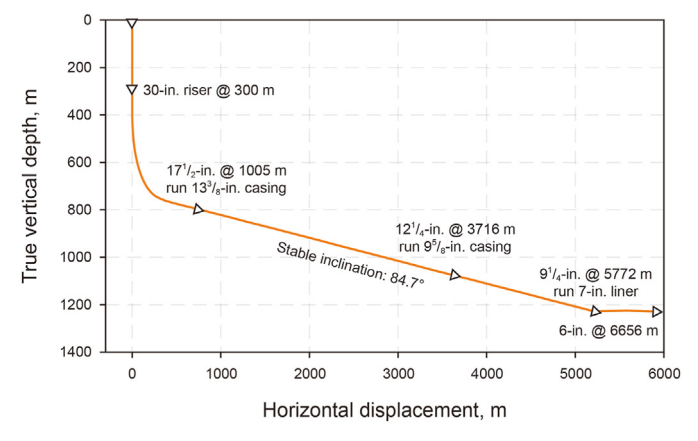


Fig. 6. Profile and structure of well X.

Table 1Basic parameters for calculation.

Categories	Parameters	Symbols	Values	Units
Wellbore	Hole diameter	d _w	0.31115	m
	Pipe outer diameter	d_{o}	0.1397	m
	Inclination	α	0-90	۰
	Pipe eccentricity	e	$e_{ m max}$	_
Drilling fluid	Density	$ ho_{ m f}$	1170	kg/m ³
	Consistency coefficient	K_{f}	0.5	Pa·s ⁿ
	Liquidity index	n_{f}	0.68	_
Cuttings	Density	$\rho_{\rm c}$	2500	kg/m ³
	Diameter	$d_{\rm c}$	0.005	m
Friction factor	Cased hole	μ_1	0.15	_
	Open hole	μ_2	0.20	_
Drilling parameters	Rotational speed	RPM	120	rev/min
	Flow rate	Q_{f}	40-80	m ³ /s
	Rate of penetration	ROP	20-70	m/h

5.1. Characteristics of dynamic cuttings transport

Firstly, the distribution of cuttings bed with time under constant parameters is simulated. As shown in Fig. 7(a), with the increase of time, the dimensionless height of cuttings bed in the wellbore gradually increases first, and then stabilizes after reaching a certain value. As shown in Fig. 7(b), the bed height in highly inclined section is almost the same when $t=7200\,\mathrm{s}$. Meanwhile, the distribution range of cuttings bed continues to expand until they fill the entire wellbore.

However, the drilling parameters will be adjusted in real-time to accommodate the change of downhole conditions in the actual drilling process, and further effecting the dynamic transport characteristics of cuttings. Therefore, the cuttings distribution in extended-reach well is usually not uniform, but rather fluctuating, which is consistent with the views of Sifferman and Becker (1992).

Fig. 8 shows the effect of the change in *ROP* on dynamic cuttings transport when other parameters remain unchanged. Firstly, drilling at a *ROP* of 50 m/h for half an hour. As shown in Fig. 8(a), within a range of about 400 m from the bottom of the well, a cuttings bed I has been formed with a height of about 26.5%.

Then, the *ROP* is reduced to 30 m/h and continue to drill for half an hour. As shown in Fig. 8(b), the height of the newly formed cuttings bed II has decreased to approximately 16.7%. At the same time, the previously formed cuttings bed I has been continuously transported upwards for about 600 m and formed a wave peak. The maximum height and well depth of the peak is about 25% and 2640 m, respectively.

Thirdly, the *ROP* is restored to 50 m/h and drilling again for half an hour. It can be found in Fig. 8(c) that the cuttings bed has shown a wavy distribution in the wellbore, including 1.5 peaks and one trough. Furthermore, under the scouring effect of drilling fluid, the maximum height of cuttings bed I also continuously drops during the transport process. In Fig. 8(c), it has decreased from 26.5% to 23.6%. Meantime, due to the height of cuttings bed II is relatively low, its transport velocity is higher than cuttings bed I. Thus, part of it has merged with cuttings bed I, and the minimum bed height at the trough is about 18%, slightly higher than the bed height formed under a *ROP* of 30 m/h.

Fourthly, the *ROP* is reduced to 30 m/h again, and then drilling for half an hour. Fig. 8(d) shows that the wavy distribution of cuttings bed is more obvious, including two integral peaks and one trough. In addition, it can be seen from in Fig. 8 that the effect of the change in *ROP* on cuttings transport has a certain delay effect, that is, the change of *ROP* occurs instantaneously. However, due to the slow transport velocity of cuttings bed, the change in *ROP* in a short period of time can only affect the cuttings transport near the

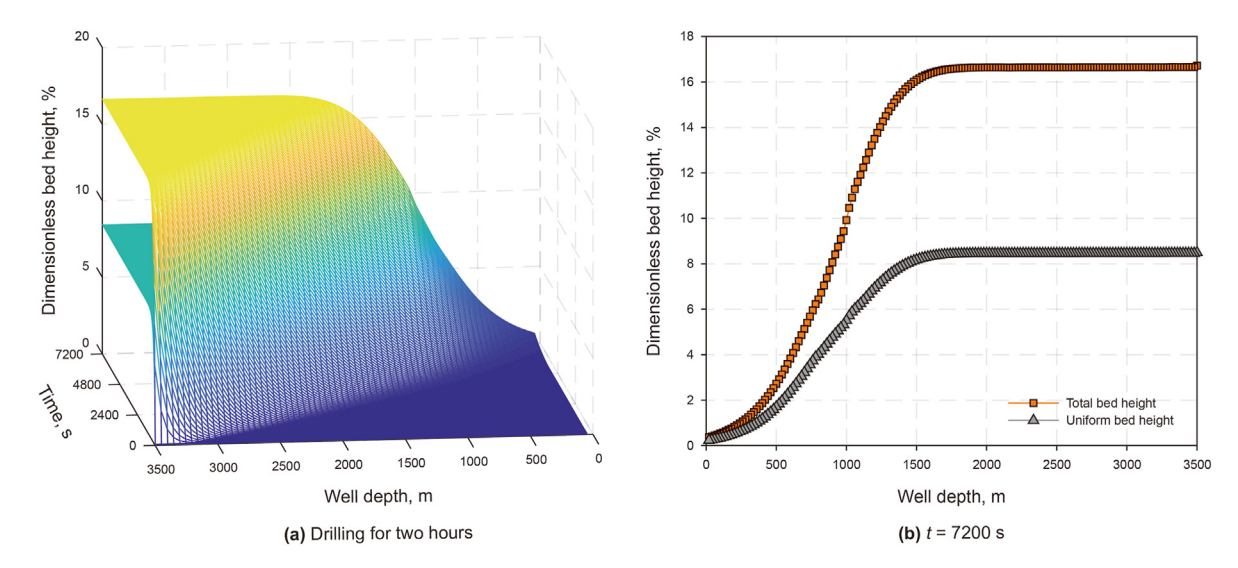


Fig. 7. Distribution of cuttings bed with time under constant parameters.

bottom of the well, but has little impact on the cleanliness of the entire wellbore. Only when the time is long enough, the influence of ROP change on cuttings distribution is significant.

The effect of the change in flow rate on dynamic cuttings transport is similar, as shown in Fig. 9. Under low flow rate, a high cuttings bed is formed. After converting to high flow rate, the height of formed cuttings bed is relatively low. In this alternating and reciprocating process, the cuttings bed shows an irregular wavy distribution in the wellbore.

In fact, the construction process of extended-reach well is not just about drilling, but also includes other operations, such as circulation, back reaming, etc. For example, after drilling each column, it is usually necessary to cycle for a certain period of time to clear the wellbore, and then make connection to continue drilling. In addition, due to the difficulty of carrying cuttings in highly deviated well sections of extended-reach well, a long cycle is usually required to fully enhance the hole cleaning after continuous drilling for a certain length (such as 500 m). Once it is believed that the wellbore cleanliness is poor or pipe sticking occurs frequently, the back reaming will be conducted to completely break through the cuttings bed in the wellbore.

The conversion of drilling operations also has a significant impact on the dynamic cuttings transport. Zhu et al. (2021) believed that the wavy distribution of cuttings bed results from the iteration of drilling and circulation. The research in this paper also supports this viewpoint. Here, a virtual drilling process where drilling and circulation alternate is assumed to analyze the effect of changes in drilling operations on the dynamic transport of cuttings.

Fig. 10 shows the characteristics of dynamic cuttings transport during the conversion process between drilling and circulation. Firstly, after drilling for half an hour, a cuttings bed formed with a height of about 26.5%, as shown in Fig. 10(a). Then, stop drilling and circulate for half an hour. Compared to Figs. 8 and 9, the difference is that there are no new cuttings generated. Under the erosion of drilling fluid, the height of cuttings bed at the bottom of the well will be gradually decreased to 0. Thus, a short well section where there are no cuttings bed eventually appears, as shown in Fig. 10(b). And the previous cuttings bed is moved up a certain distance. Repeating the above process, the cuttings bed shows distinct wave distribution, and the maximum bed height is also reduced to the greatest degree possible. For the cuttings bed generated during the first drilling, its maximum bed height has decreased from 26.5% to

21.3% in Fig. 10(c) and 19.2% in Fig. 10(d). This indicates that circulating drilling fluid can effectively reduce the accumulation of cuttings in the wellbore and significantly improve hole cleaning.

Overall, the height of cuttings bed in extended-reach well is not a constant predicted by steady model, but varies with the drilling parameters like *ROP*, flow rate, rotational speed, etc., as well as drilling operations. The established transient model for cuttings transport can capture the detailed transport characteristics of cuttings, demonstrating the superiority of this model and its ability to better predict the dynamic cuttings transport over time.

5.2. Analysis of the drilling process

The authors' previous study (Zhao et al., 2024) had found that the change in drilling parameters will affect hole cleaning, and further affect the torque loss caused by cuttings. This explains that the ground torque decreases with well depth in some cases, rather than showing a normal increasing trend.

However, the changes in drilling parameters occur instantaneously, but the changes in cuttings bed distribution are slow due to low transport velocity of cuttings bed. As mentioned earlier in this paper, the effect of the change in drilling parameters on cuttings transport has a certain delay effect. Therefore, coupling the tubular mechanical behaviors with transient cuttings transport model can more accurately simulate and analyze the impact of wellbore cleanliness on the ground torque during rotary drilling.

When drilling from 3060 to 3170 m, the change in flow rate has an impact on the ground torque, as shown in Fig. 11. When the flow rate decreased from 64 to 63 L/s, the worse hole cleaning leads to higher torque loss, so the ground torque increases at a higher slope. While the flow rate increased from 63 to 66 L/s, the improved hole cleaning make the torque loss reduce, so the ground torque remains unchanged or even decreases with the well depth.

According to Fig. 11, both steady and transient models for cuttings transport can capture these abnormal phenomena, but the change in ground torque is completely synchronized with the change in flow rate under steady model, while the transient model can reflect the delay effect of change in ground torque, which is more in line with the actual situation. The delay length is 5–25 m, corresponding to a delay time of approximately 10~30 min. Moreover, once the effect of cuttings is neglected, the ground torque will be greatly underestimated.

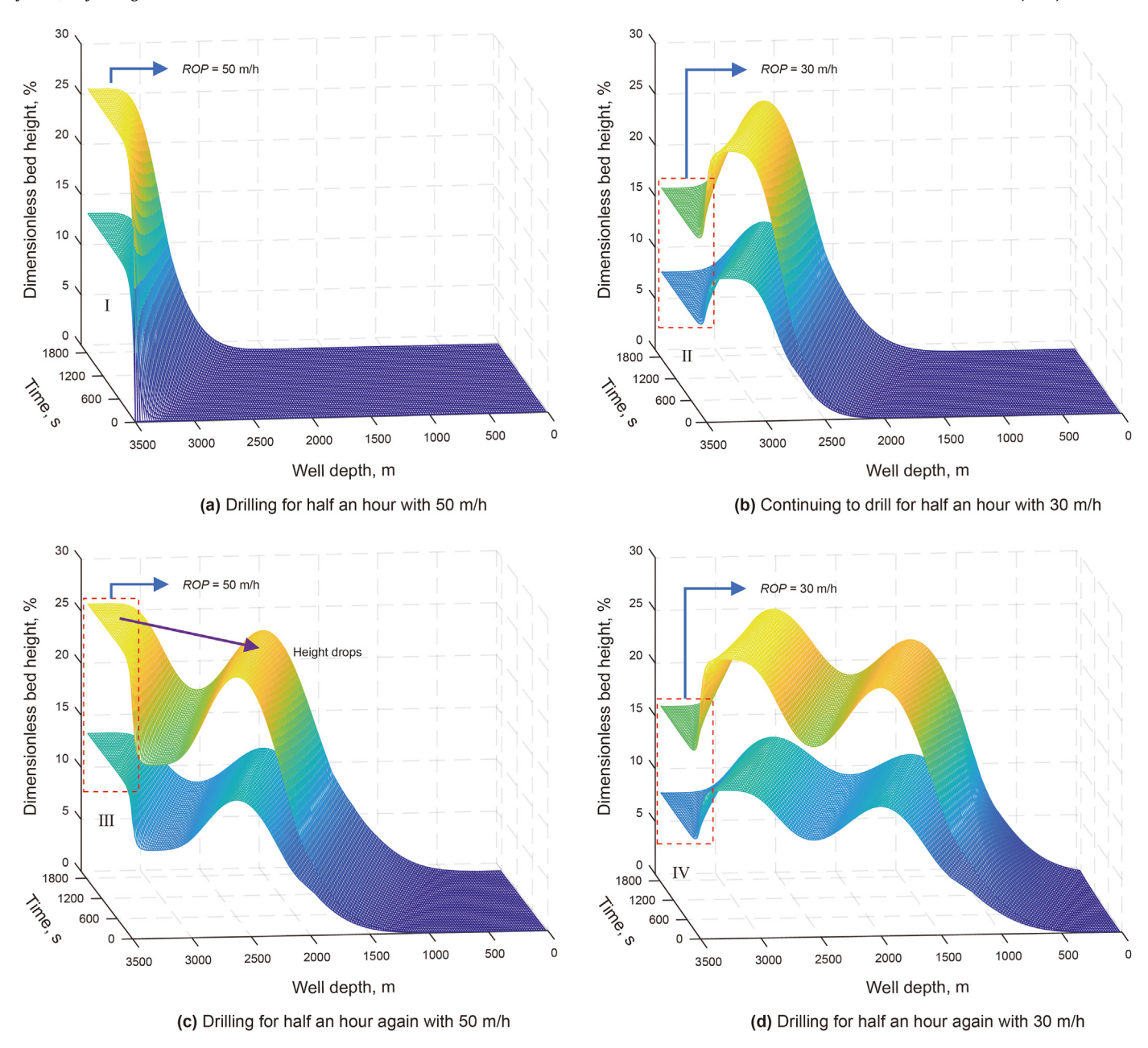


Fig. 8. Effect of the change in ROP on dynamic cuttings transport.

When drilling from 3315 to 3480 m, the *ROP* continuously varies within 25–50 m/h, which dominates the synchronous fluctuations of the ground torque, as shown in Fig. 12. Similarly, under steady model, the ground torque is completely synchronized with the *ROP*. In fact, there is a certain delay effect between the change in measured ground torque and the change in *ROP*. The delay length and delay time are 20–30 m and 25–40 min, respectively. And the transient model can describe this finely phenomenon.

For the $12^1/_4$ -in. Section, the first drilling ended at 2750 m. Before tripping out the tubular string, sufficient circulation and back reaming was conducted to clean the wellbore. Therefore, the cuttings bed was considered non-existent at the beginning of the second drilling. During the second drilling, the measured and predicted ground torques are shown in Fig. 13. Overall, the effect of cuttings on the ground torque is significant and non-negligible, and the predicted ground torque under the transient model shows

better consistency with the measured data.

5.3. Optimization of drilling procedures

5.3.1. Optimization of ROP

In Section 5.1, the effect of the change in *ROP* on dynamic cuttings transport has been simulated and discussed. Although high *ROP* can save time and cost, it is not conducive to hole cleaning. Therefore, it is not advisable to use high *ROP* for long-term drilling. In fact, on site construction also recognized this phenomenon. During drilling $12^1/_4$ -in. Section, there was a frequent conversion between high *ROP* and low *ROP* (as shown in Fig. 14), so as to improve hole cleaning as much as possible. Here, the well section through which the *ROP* increases from a minimum value to a maximum value and then decreases to another minimum value is defined as one adjustment period, and the range between the

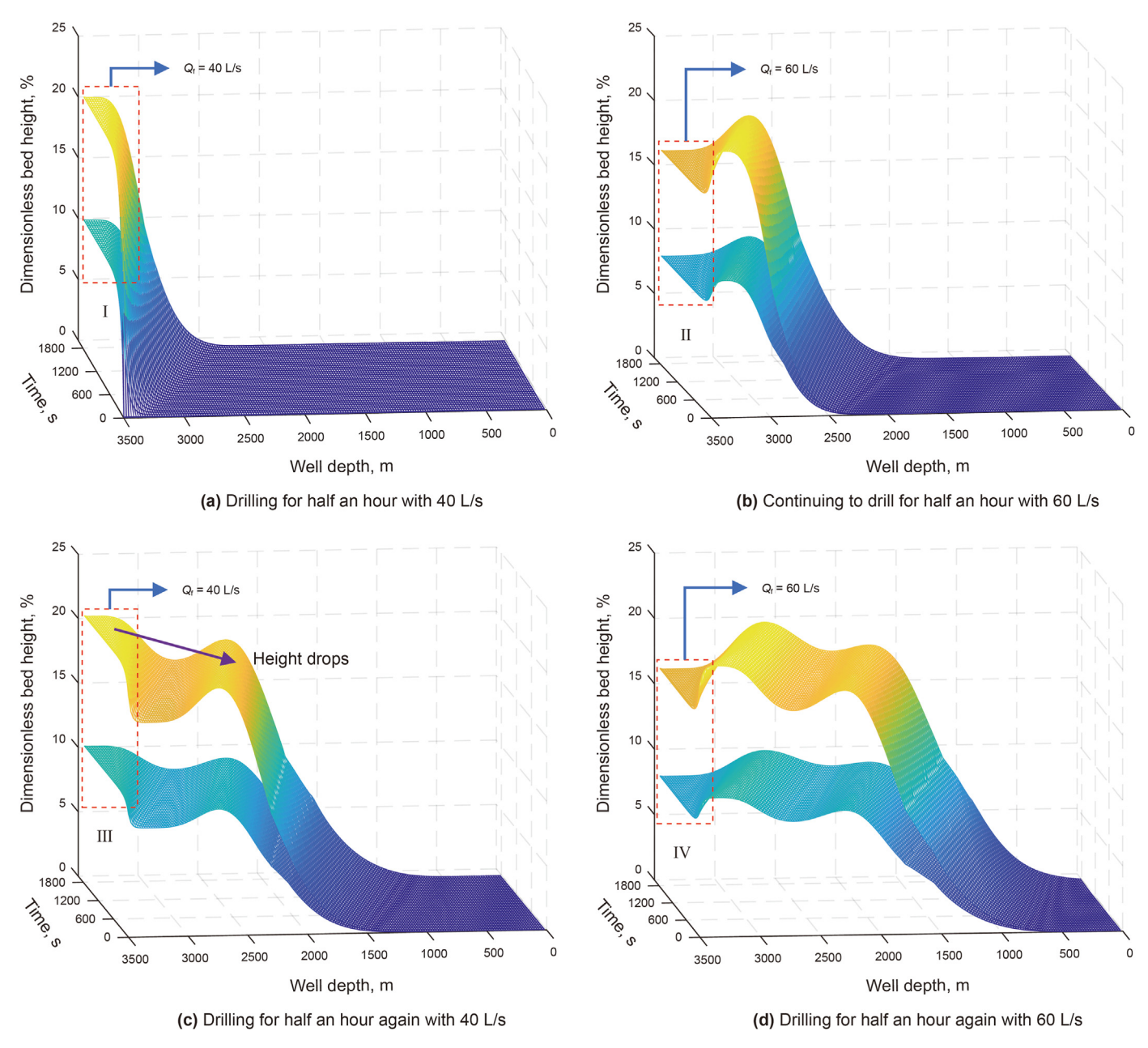


Fig. 9. Effect of the change in flow rate on dynamic cuttings transport.

minimum *ROP* and *ROP* in an adjustment period is defined as the adjustment range. For well X, the adjustment period is about 20–70 m, and the adjustment ranges are mainly in 30–60 m/h according to Fig. 14.

In actual drilling, it is basically impossible to maintain a constant *ROP*, and the *ROP* always fluctuates. Below, the adjustment period and adjustment range for the *ROP* are optimized. It can be compared to the vibration of tubular string. In the early days, all vibrations were considered harmful. However, through researches and drilling practices, it was found that actively controlling the vibration phenomenon of the tubular string can effectively reduce axial friction, thereby alleviating the problem of backpressure in horizontal section (Shi et al., 2023a, 2023b). The optimization of *ROP* here is similar.

The adjustment period for *ROP* is taken as 30–60 m/h. After drilling 6-fold adjustment period (fully reflect the impact of

adjusting *ROP*), the distributions of cuttings bed along the wellbore under different adjustment periods are shown in Fig. 15(a). Firstly, it can be found that adopting a constant *ROP* (mean value of 45 m/h) is not the optimal drilling scheme.

Secondly, when the adjustment period is 0.44 h (20 m), the hole cleaning is best and the bed height in highly inclined section is relatively uniform. If the adjustment period increases, the cuttings bed shows wavy distribution, including two large sand dunes. For example, when the adjustment period is 1.11 h (50 m), the formation of dunes occurred between 1000–2000 m and 2000–3500 m, respectively. While the adjustment period is more than 1.56 h (70 m), there is only one sand dune in the wellbore due to the limitation of well depth, resulting in high cuttings bed in the entire highly inclined section.

During this virtual drilling process, the maximum torque loss caused by cuttings is shown in Fig. 15(b). It can be found that the

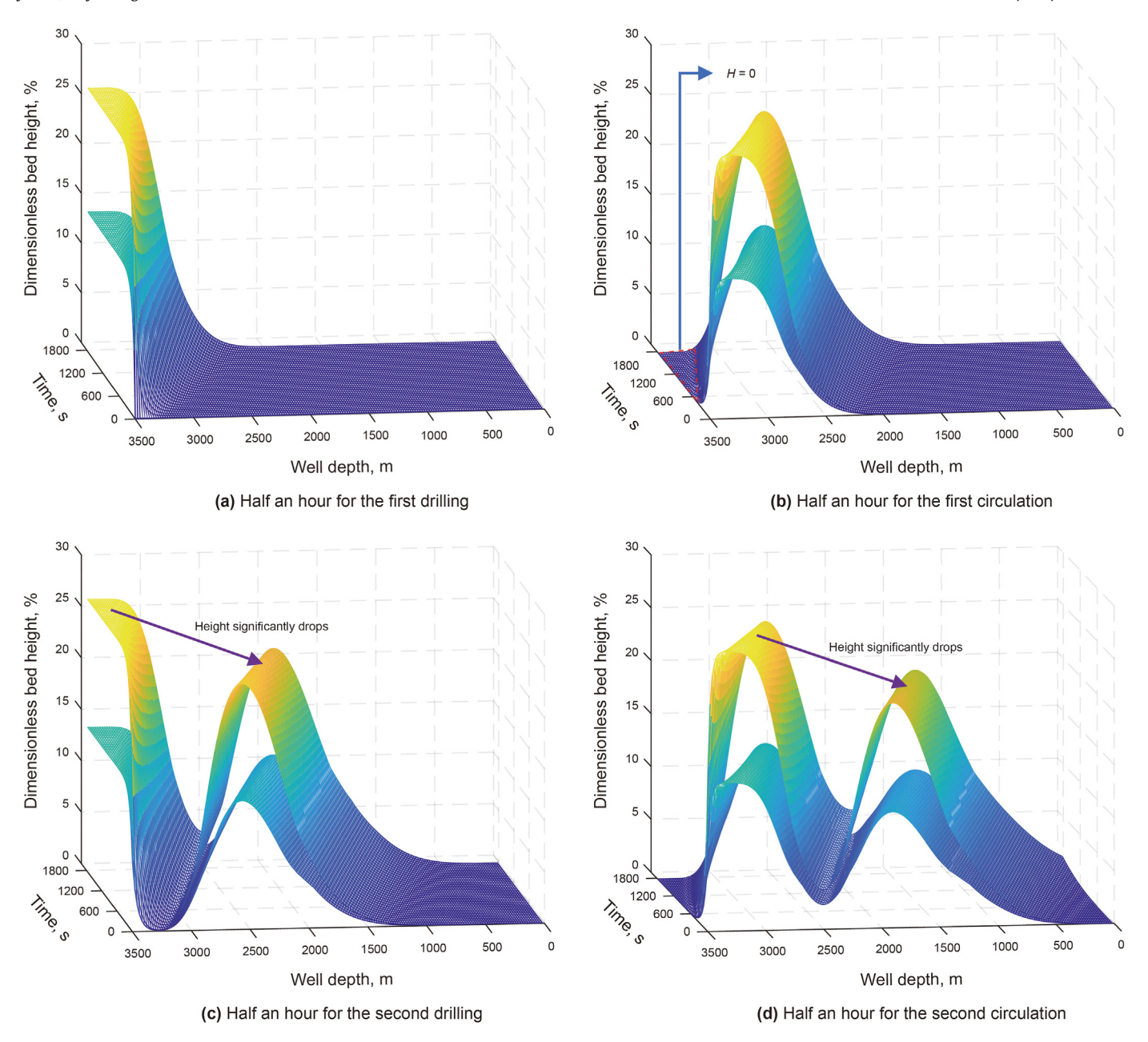


Fig. 10. Effect of the change in drilling operations on dynamic cuttings transport.

short adjustment period is the best. When the adjustment period is 0.44 h, the torque loss caused by cuttings is only 2.54 kN·m. Furthermore, the torque loss caused by cuttings does not increase continuously with the adjustment period, and there is a minimum value at 1.44 h. Therefore, if the rapid adjustment for ROP cannot be achieved, the recommended adjustment period for ROP is 1.44 h when the well depth is 3500 m. This can not only reduce the frequency of adjusting ROP, but also avoid excessive torque loss caused by cuttings.

In addition, the whole influence of the adjustment period on cuttings bed distribution is not fully demonstrated at small well depth. Specifically, before the end of an adjustment period, the earlier generated cuttings bed may have been transported to the wellhead. Thus, the effect of the total well depth on the recommended adjustment period cannot be neglected. Based on the calculation results, the recommended adjustment period for *ROP* is

not constant, but increases with the total well depth increases, as shown in Fig. 16. This also explains that the adjustment period for *ROP* during drilling 2750–3100 m is smaller than that of during drilling 3100–3500 m, as shown in Fig. 14.

Taking the adjustment period for *ROP* as 1.44 h, the distributions of cuttings bed under different adjustment ranges are shown in Fig. 17. When the mean value of the *ROP* is the same, the maximum bed height is higher and its wavy distribution characteristics are more evident under wider adjustment range, as shown in Fig. 17(a). For example, there is a large dune in 1300–3500 m when the adjustment range for *ROP* is 20–70 m/h. In 2000–2500 m, the bed height is more than 25%, indicating high risk of pipe stuck. Thus, the large-scale adjustment range for *ROP* should be avoided as much as possible.

When the scale of the adjustment range for *ROP* is the same, lower *ROP* is more profit for hole cleaning, as shown in Fig. 17(b).

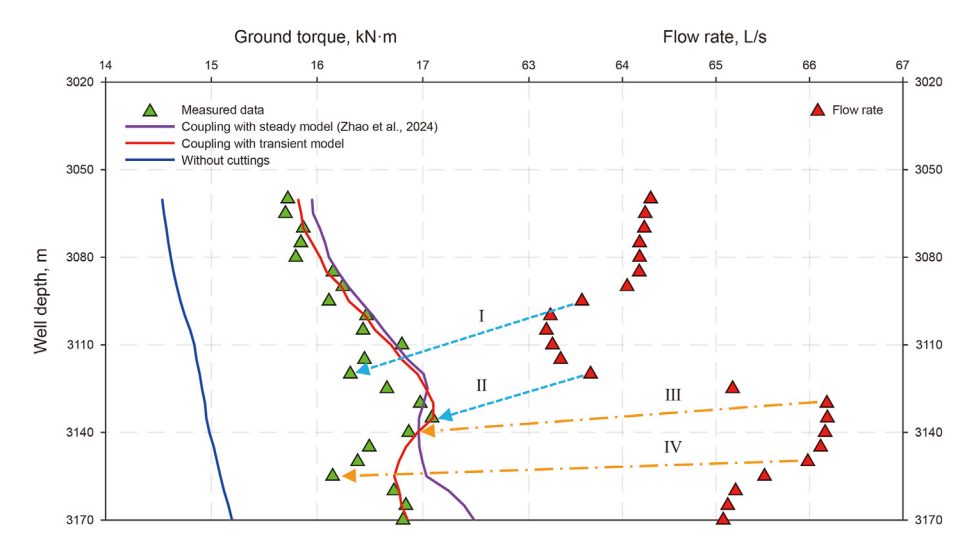


Fig. 11. Effect of the change in flow rate on the ground torque.

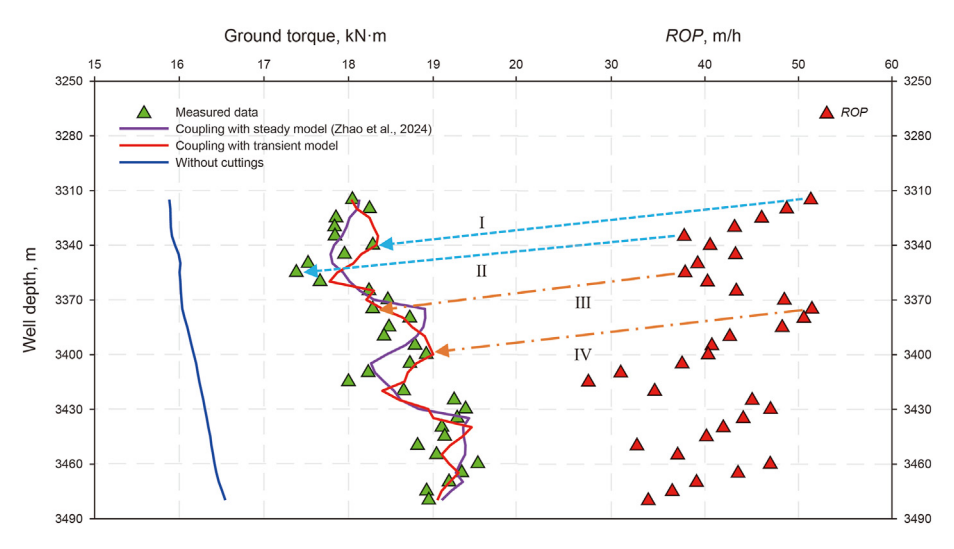


Fig. 12. Effect of the change in ROP on the ground torque.

Overall, the best way is to make small-scale adjustments for *ROP* at a low level.

Fig. 18 shows the torque loss caused by cuttings under different adjustment ranges. Combining Figs. 17 and 18, the recommended optimal adjustment range for *ROP* is 30–40 m/h, that is, making small adjustments to the *ROP* can ensure better hole cleaning and minimize the torque loss caused by cuttings. If the drilling efficiency should be improved, the recommended adjustment range for *ROP* are 30–50 and 40–50 m/h. In fact, 30–40 and 40–50 m/h are the most frequently applied adjustment ranges during the second drilling in $12^1/_4$ -in. Section of well X. Theoretical analysis and empirical understanding of on-site operations achieves unity, which indirectly verifies the accuracy of the theoretical models.

5.3.2. Optimization of flow rate

Increasing the flow rate during drilling can also improve the hole cleaning. For example, when drilling to 3120 m, the flow rate is increased to 66 L/s to enhance the hole cleaning, as shown in Fig. 11. However, the key problem is how long the most appropriate drilling time is after increasing the flow rate.

Fig. 19(a) shows the cuttings bed distribution under different drilling time with increased flow rate (ROP = 40 m/h). Obviously, only a part of cuttings bed is affected by the increased flow rate in the short term. For example, when the drilling time is 0.75 h (30 m), namely drilling from 3100 to 3130 m, the cuttings bed in 2500–3100 m is fully affected, the cuttings bed in 1800–2500 m is affected to a certain extent, while the cuttings bed in the well section below 1000 m is not affected.

Fig. 19(b) shows the variation of torque loss caused by cuttings in the range of 0–3100 m with drilling time. It can be found that the torque loss caused by cuttings will no longer continue to decrease if the drilling time is more than 1.75 h. Therefore, the recommended drilling time for the increased flow rate is 1.75 h, indicating that the cleanliness in the entire wellbore has been fully improved.

The optimal drilling time is also closely related to the total well depth. With the increase of the total well depth, the distance of upward cuttings transport also increases. Thus, more time are needed to fully enhance the hole cleaning. As shown in Fig. 20, the recommended drilling time increases linearly with the total well depth.

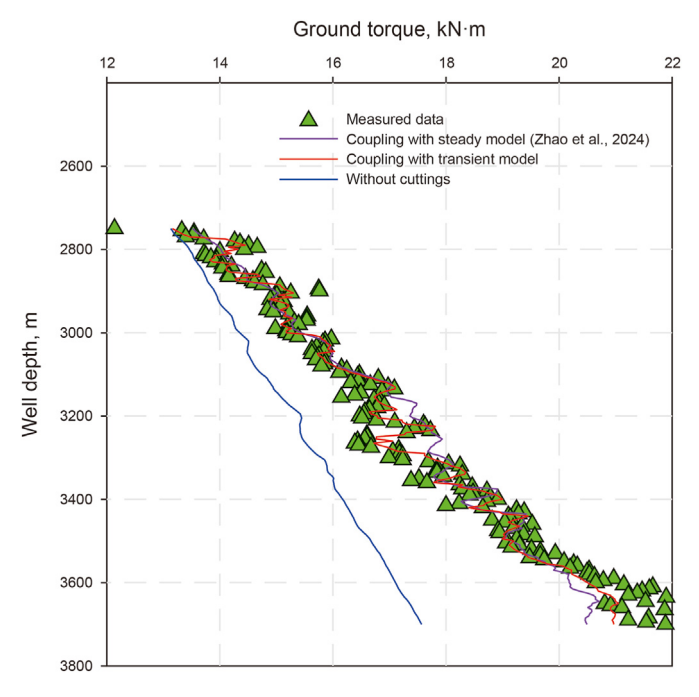


Fig. 13. Ground torques with well depth.

5.3.3. Optimization of circulation

During the drilling process, enough hole cleaning cannot be always ensured by adjusting drilling parameters. If the hole cleaning is quite poor or it has been continuously drilling for a long well section, circulation will usually be carried out to significantly improve the wellbore cleanliness. In this section, the time interval between the two adjacent circulations and the time of each circulation are optimized.

Assuming that there is no cuttings bed in the wellbore at t = 0 s, the adjustment period and range for the *ROP* are 1.44 h and 40–50 m/h, respectively, and the flow rate is the mean values of the measured data, i.e., 63.5 L/s. The cuttings bed distribution under different drilling times is shown in Fig. 21.

During the drilling, about 3 h later, there are relatively high cuttings bed throughout the entire highly inclined section, as shown in Fig. 21(a). Therefore, it is recommended to conduct a circulation after continuous drilling for 3 h.

During the circulation, about 2.1 h later, the maximum cuttings bed height in the wellbore is smaller than 10%, as shown in Fig. 21(b). According to Eqs. (31) and (32), the contact force result from cuttings can be neglected when the bed height is below 10%. Therefore, it is recommended that the time of each circulation is no less than 2.1 h.

With the increase of the total well depth, more time is needed for the cuttings bed to fill the entire highly inclined section in drilling, while circulation requires cleaning the cuttings bed in longer well section. Thus, the circulation interval and the time of each circulation also increase, as shown in Fig. 22.

5.3.4. Optimization of back reaming

In some cases, back reaming is necessary to be conducted to thoroughly clean the wellbore. After stopping drilling, it is recommended not to immediately carry out back reaming, but to firstly cycle for a period of time. This is because the size of the BHA is larger than drill pipe, if the back reaming is performed immediately, BHA will scrape and pull the cuttings bed. Under the "bull-dozer effect", it may cause serious local accumulation of cuttings near the BHA (Chen et al., 2023; Zhu et al., 2023), leading to the risk of pipe stuck.

Under different initial height of cuttings bed, the effect of circulation time on cuttings bed height is shown in Fig. 23. It can be found that the cuttings bed has been cleaned when the circulation time is 1200 s (20 min). Thus, it is recommended to firstly cycle for

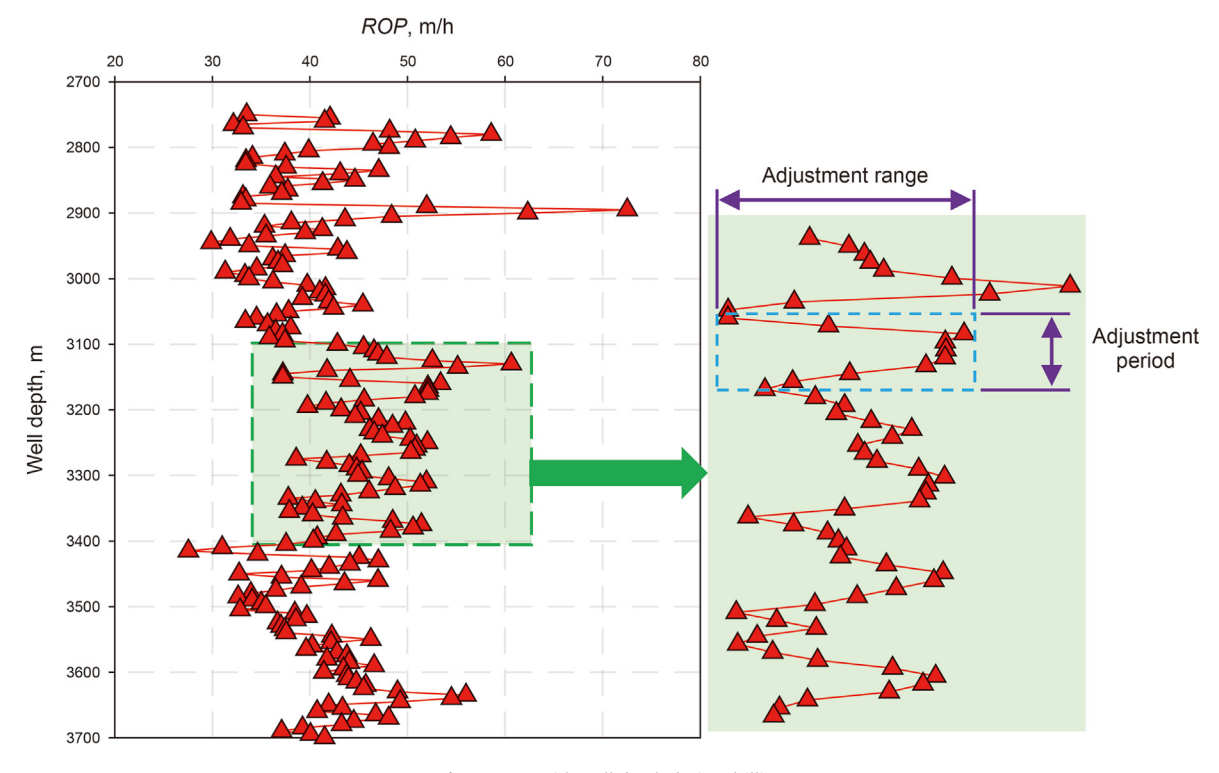


Fig. 14. ROP with well depth during drilling.

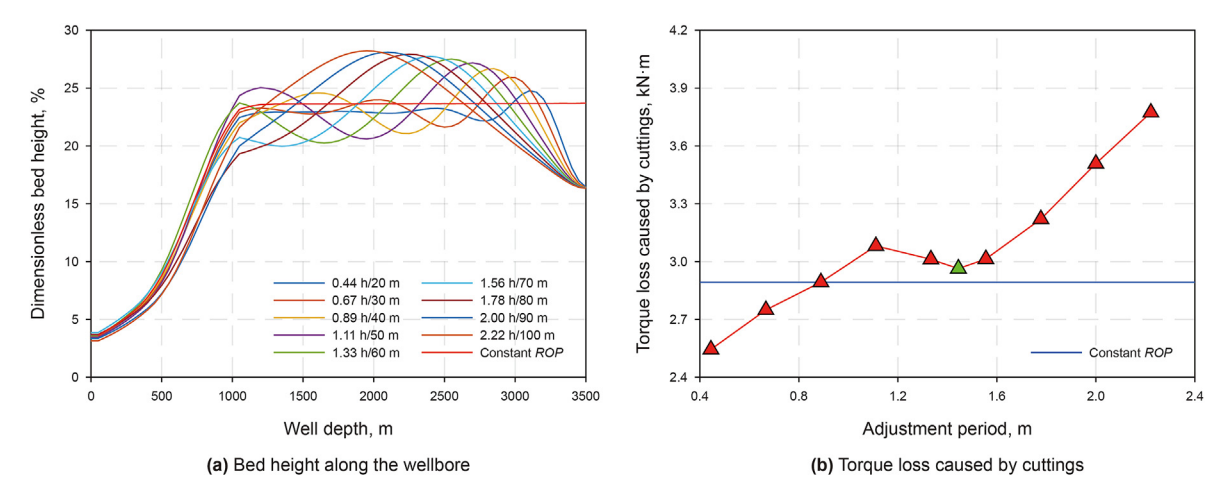


Fig. 15. Optimization of adjustment period.

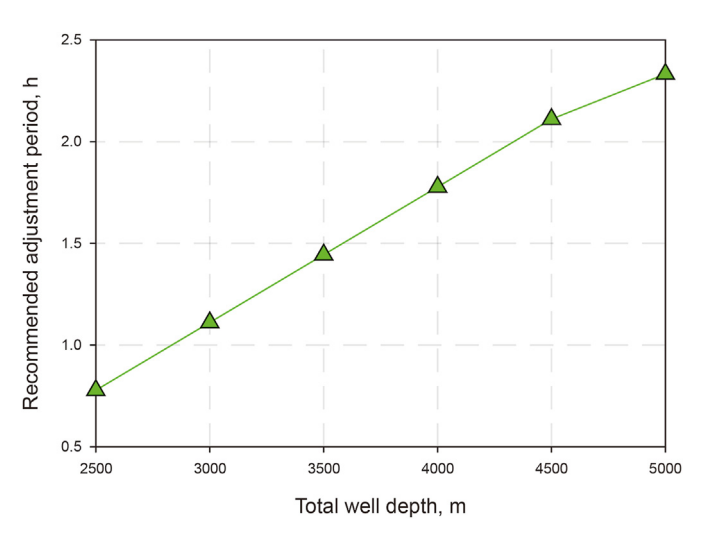


Fig. 16. Recommended adjustment period with the total well depth.

at least 20 min before back reaming.

For back reaming, the velocity is crucial. The local accumulation of cuttings bed near the connectors is one of the main reasons for tight spots when the back reaming velocity is too fast (Zhu et al.,

2023). To avoid connectors scraping and pulling the cuttings bed, the back reaming velocity has to be smaller than the minimum transport velocity of the uniform bed.

Fig. 24(a) shows the distributions of cuttings bed and its velocity in the wellbore after drilling at a *ROP* of 40 m/h for 0.5 h and then circulation for 0.5 h. At the thickest position of the uniform bed, its

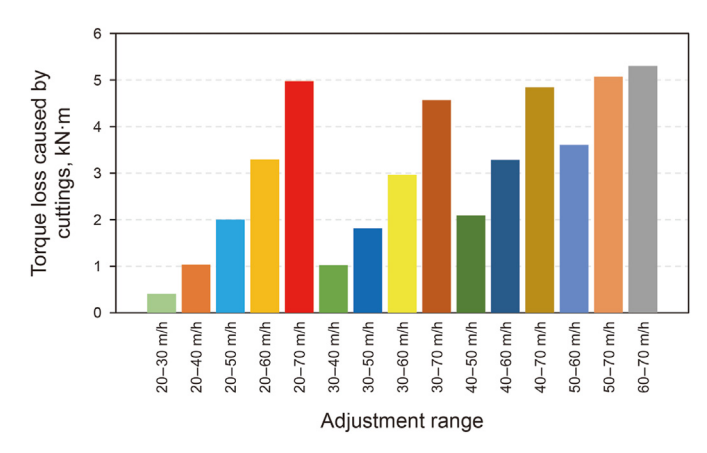


Fig. 18. Torque loss caused by cuttings under different adjustment ranges.

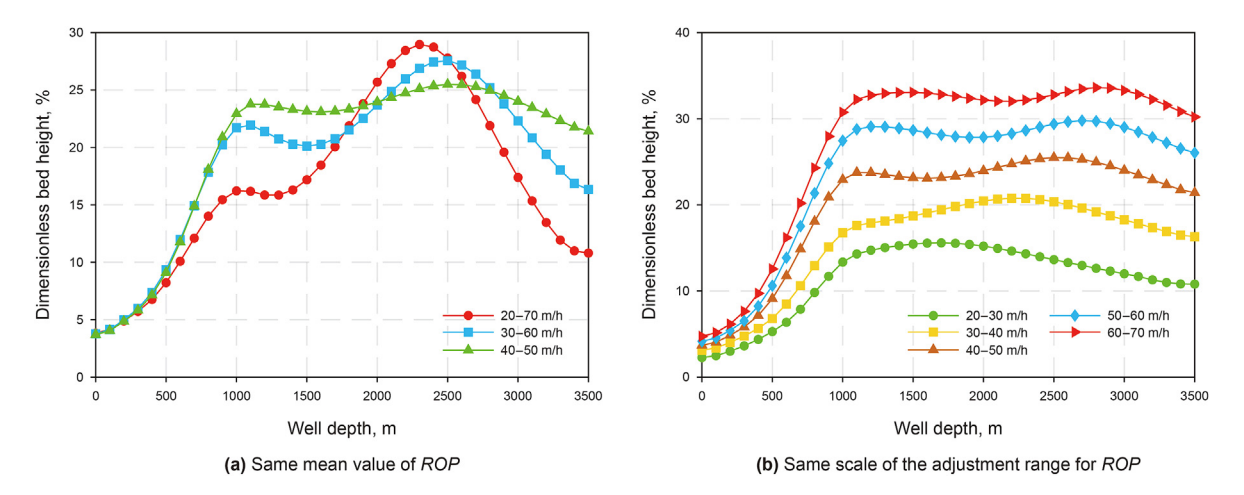


Fig. 17. Effect of adjustment range on cuttings bed distribution.

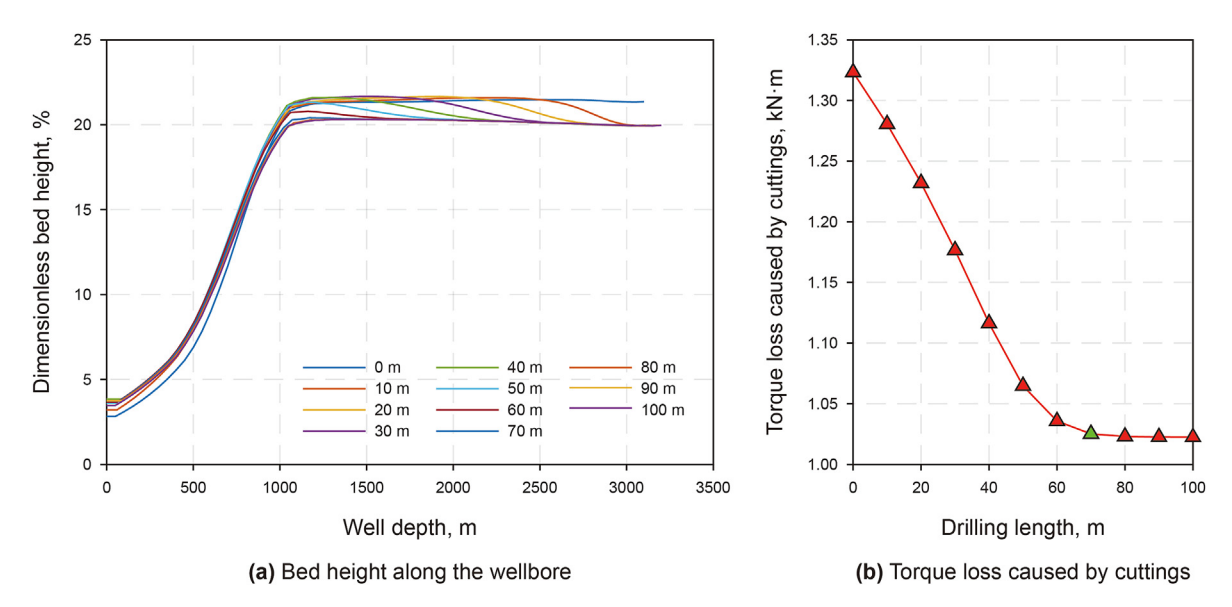


Fig. 19. Optimization of drilling time after increasing the flow rate.

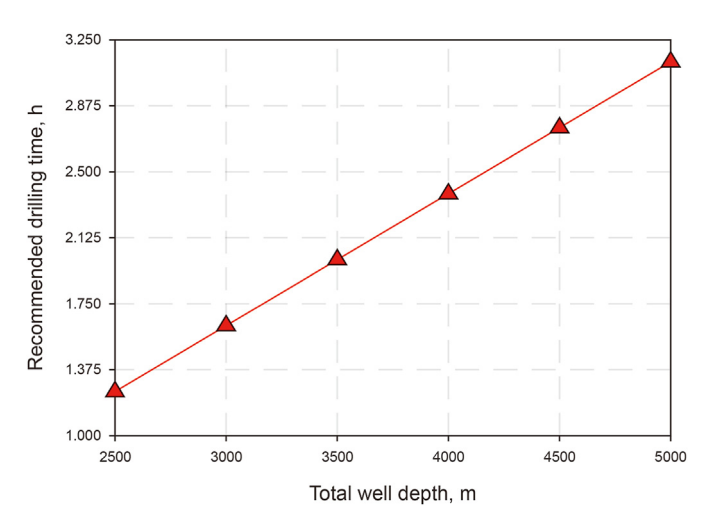


Fig. 20. Recommended drilling time with the total well depth.

transport velocity is the smallest. Similarly, there is also a minimum transport velocity of uniform bed in the wellbore during back reaming. For conservatism, 50% of this minimum transport velocity is considered as the maximum back reaming velocity.

Fig. 24(b) shows that the maximum back reaming velocity increase with the flow rate. For example, when the initial bed height is 20%, the maximum back reaming velocity increases from 0.026 (about 3.09 columns per hour) to 0.060 m/s (about 7.15 columns per hour) while the flow rate is increased from 50 to 70 L/s. And the maximum back reaming velocity decreases with the initial bed height. For example, when the flow rate is 60 L/s, the maximum back reaming velocity decreases from 0.066 (about 7.94 columns per hour) to 0.043 m/s (about 5.21 columns per hour) while the initial bed height is increased from 10% to 25%.

Moreover, there is a minimum flow rate for the back reaming. For example, when the initial bed height is 20%, the uniform bed will convert into the stationary bed once the flow rate is smaller than 50 L/s, indicating extremely high risk of pipe stuck when carries out back reaming in this situation.

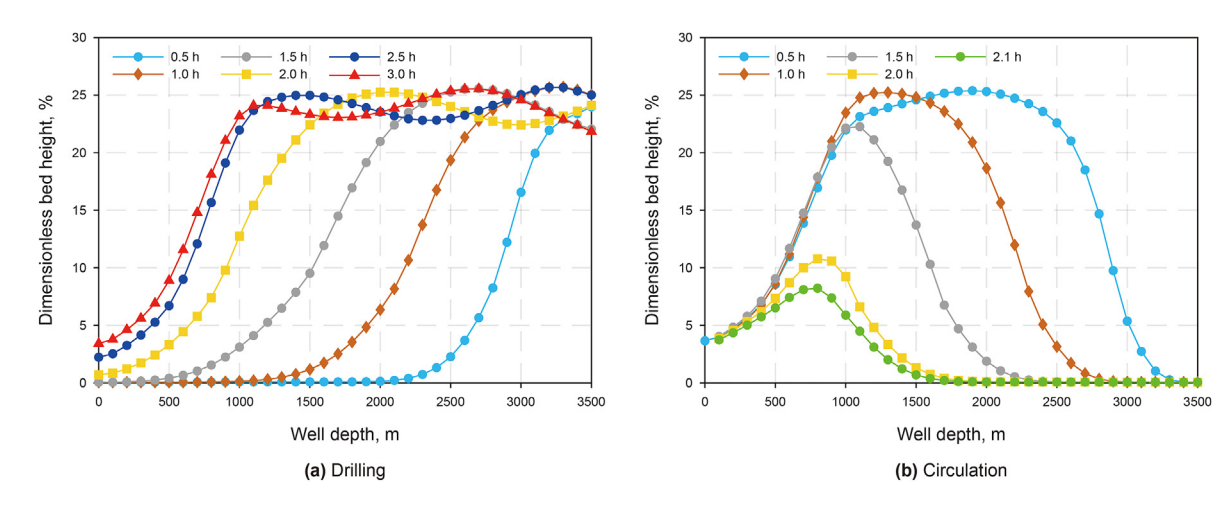


Fig. 21. Cuttings bed height while drilling and circulation.

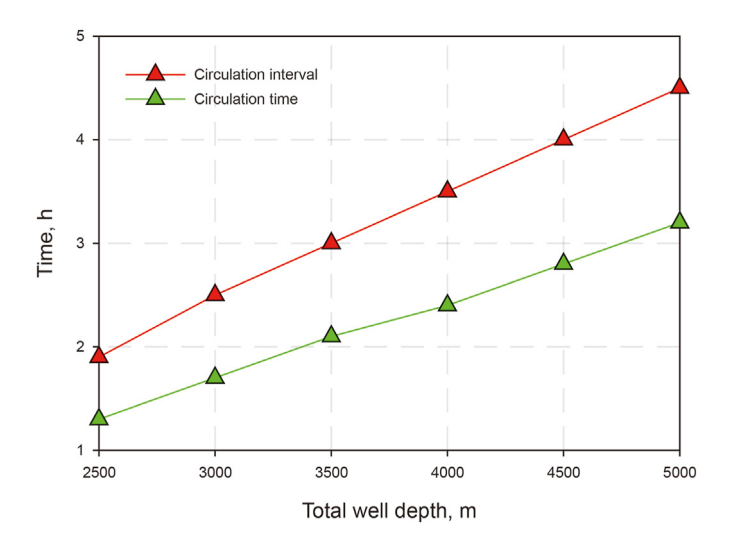


Fig. 22. Effect of the total well depth on circulation.

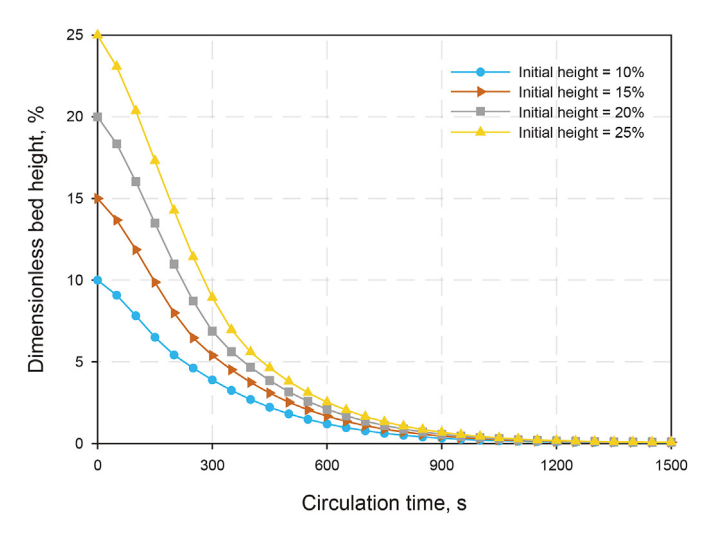
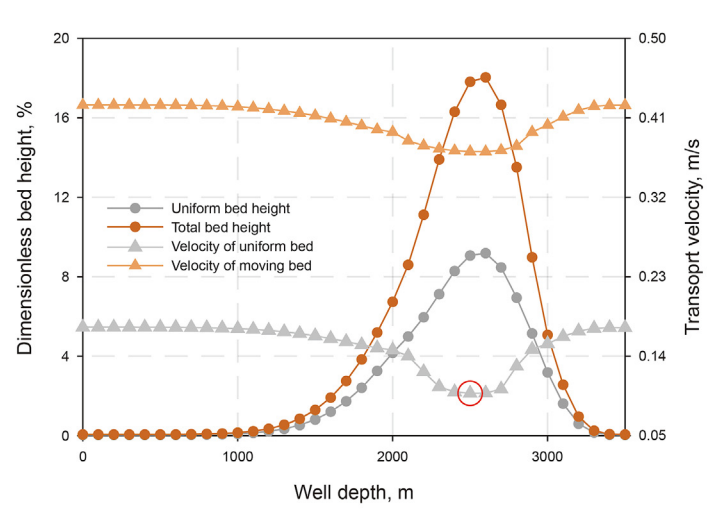


Fig. 23. Effect of circulation time on cuttings bed height under different initial height.



(a) Bed height and its transport velocity

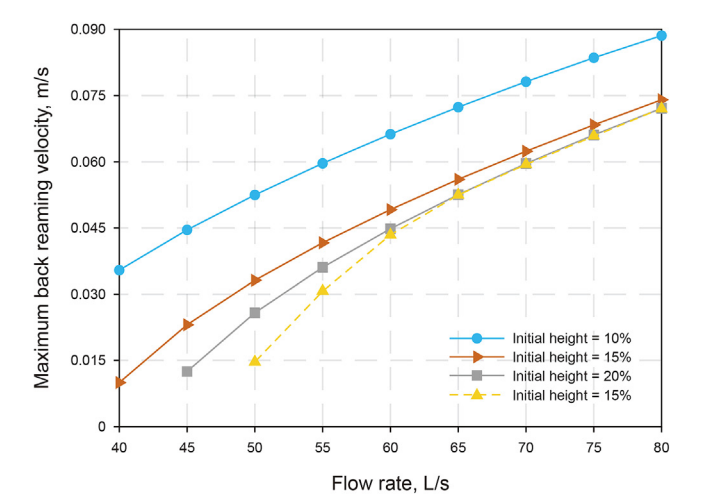
6. Limitations and recommendations for future work

- (1) The theoretical models are mainly validated through experiments, but experiments cannot simulate complicated downhole conditions. Therefore, it is necessary to strengthen the collection of relevant data on cuttings transport during the drilling process. For example, record the size, shape, concentration, and quality of collected cuttings at the surface. And to further validate the accuracy of the theoretical model and correct its parameters through these data, so as to more accurately predict the hole cleaning in extended-reach drilling.
- (2) The temperature of drilling fluid will change with well depth, which in turn affects the performance of the drilling fluid and its capacity of carrying cuttings. Therefore, cuttings transport models considering the influence of temperature changes should be further established.
- (3) The researches on cuttings transport mainly focuses on solid-liquid two-phase flow, and there is less research on the gas-liquid-solid three-phase flow. For example, the fluid and gas jointly control the cuttings transport during managed pressure drilling. Thus, it is necessary to conduct research on the cuttings transport under three-phase flow conditions.

7. Conclusions

Based on the above studies, the following conclusions can be drawn.

- (1) In extended-reach drilling, the real-time adjustment of drilling parameters like *ROP* and flow rate, will affect the characteristics of dynamic cuttings transport, leading to the non-uniform distribution of cuttings bed in highly inclined section. Similarly, the change in drilling operations can also affect the characteristics of dynamic cuttings transport. For example, via the alternation of drilling and circulation, the cuttings bed shows a clear wavy distribution in the wellbore.
- (2) The changes in drilling parameters occur instantaneously, but the changes in cuttings bed distribution are slow due to low transport velocity of cuttings bed. Therefore, there is a delay effect for the effect of the changes in drilling



(b) Maximum back reaming velocity

Fig. 24. Optimization of back reaming velocity.

parameters on the ground torques, which is consistent with the actual drilling process. Through the coupling analysis of transient cuttings transport and tubular mechanical behaviors, it can not only accurately simulate the evolution of the downhole conditions over time, but also capture the delay effect of ground torques, thereby providing a solid theoretical basis for optimizing drilling procedures.

- (3) Analogous to controlling the vibration of tubular string to improve drilling efficiency, the adjustment period and adjustment range for the *ROP* are optimized to improve the hole cleaning and reduce the torque loss caused by cuttings. For example, when the total well depth is 3500 m, the recommended adjustment period for *ROP* is no more than 1.44 h, and the recommended range for *ROP* are 30–40 m/h and 40–50 m/h.
- (4) Due to the time delay effect of the changes in drilling parameters on the cuttings transport, the optimal drilling time for increasing the flow rate from low level to high level is optimized, so as to make the impact of high flow rate to be transmitted from the bottom to the beginning of the highly inclined section. For example, when the total well depth is 3500 m, the recommended drilling time for the increased flow rate is 2.0 h.
- (5) Circulation is an important measure to hole cleaning during extended-reach drilling, and the keys are choosing appropriate time interval between the two adjacent circulations and the time of each circulation. In this paper, the time required from non-existent cuttings bed to cuttings bed being filled with the entire highly inclined section is considered as the most appropriate time interval, and the time required for reducing the maximum bed height in the wellbore to less than 10% is considered as the most appropriate time for each circulation.
- (6) To avoid pipe stuck, it is necessary to cycle for at least 20 min to remove the cuttings bed near the large-sized BHA before back reaming, and the maximum back reaming velocity should be smaller than the minimum transport velocity of the uniform bed. Moreover, there is a minimum flow rate for the back reaming. When the flow rate is smaller than this value, the uniform bed will convert into the stationary bed, indicating extremely high risk of pipe stuck.

CRediT authorship contribution statement

Jun Zhao: Writing — original draft, Validation, Software, Methodology, Investigation, Formal analysis, Conceptualization. **Wen-Jun Huang:** Writing — original draft, Validation, Resources, Project administration, Methodology, Conceptualization. **De-Li Gao:** Validation, Resources, Project administration, Funding acquisition, Conceptualization. **Wen-Long Li:** Writing — original draft, Supervision, Resources.

Declaration of competing interest

The authors declare that they have no known competing financial interests or personal relationships that could have appeared to influence the work reported in this paper.

Acknowledgments

The authors gratefully acknowledge the financial support from the Natural Science Foundation of China (Grant Nos. 52222401, 52234002, 52394255), National Key Research and Development Program of China (Grant No. 2023YFC2810901), and Science

Foundation of China University of Petroleum, Beijing (Grant No. ZXZX20230083).

References

- Chen, Y.F., Zhang, H., Wu, W.X., Li, J., Ouyang, Y., Lu, Z.Y., Dong, Z.X., 2024. Simulation study on cuttings transport of the backreaming operation for long horizontal section wells. Petrol. Sci. 21 (2), 1149–1170. https://doi.org/10.1016/ j.petsci.2023.09.021.
- Dao, N.H., Mahjoub, M., Menand, S., Nguyen, K.L., 2023. Modeling of a detailed bow spring centralizer description in stiff-string torque and drag calculation. Geoen 222, 211457. https://doi.org/10.1016/j.geoen.2023.211457.
- Doan, Q.T., Oguztoreli, M., Masuda, Y., Yonezawa, T., Kobayashi, A., Naganawa, S., Kamp, A., 2003. Modeling of transient cuttings transport in underbalanced drilling (UBD). SPE J. 8 (2), 160–170. https://doi.org/10.2118/85061-PA.
- Gavignet, A.A., Sobey, I.J., 1989. Model aids cuttings transport prediction. J. Petrol. Technol. 41 (9), 916–921. https://doi.org/10.2118/15417-PA.
- Guo, X.L., Wang, Z.M., Long, Z.H., 2010. Study on three-layer unsteady model of cuttings transport for extended-reach well. J. Petrol. Sci. Eng. 73 (1–2), 171–180. https://doi.org/10.1016/j.petrol.2010.05.020.
- Hirpa, M.M., Kuru, E., 2020. Hole cleaning in horizontal wells using viscoelastic fluids: an experimental study of drilling-fluid properties on the bed-erosion dynamics. SPE J. 25 (5), 2178–2193. https://doi.org/10.2118/199636-PA.
- Ho, H., 1988. An improved modeling program for computing the torque and drag in directional and deep wells. SPE Annual Technical Conference and Exhibition, Houston, Texas. https://doi.org/10.2118/18047-MS.
- Huang, W.J., Gao, D.L., 2019. Combined effects of wellbore curvature, connector, and friction force on tubular buckling behaviors. SPE J. 24 (5), 2083–2096. https:// doi.org/10.2118/195680-PA.
- Huang, W.J., Gao, D.L., 2021. Local-integral coupling model of tubular strings with connectors and its application in periodic sticking analyses. SPE J. 26 (6), 3410–3423. https://doi.org/10.2118/204463-PA.
- Huang, W.J., Gao, D.L., Liu, Y., 2018. Buckling analysis of tubular strings with connectors constrained in vertical and inclined wellbores. SPE J. 23 (2), 301–327. https://doi.org/10.2118/180613-PA.
- Johancsik, C., Friesen, D., Dawson, R., 1984. Torque and drag in directional wells-prediction and measurement. J. Petrol. Technol. 36 (6), 987–992. https://doi.org/10.2118/11380-PA.
- Kim, Y.J., Woo, N.S., Hwang, Y.K., Kim, J.H., Han, S.M., 2014. Transport of small cuttings in solid-liquid flow with inclined slim hole annulus. J. Mech. Sci. Technol. 28, 115–126. https://doi.org/10.1007/s12206-013-0952-7.
- Li, X., 2018. Basic Research on Prediction & Control of Maximum Measured Depth of Open Hole in Horizontal Extended-Reach Drilling. PhD Dissertation. China University of Petroleum, Beijing.
- Mahaffy, J.H., 1982. A stability-enhancing two-step method for fluid flow calculations. J. Comput. Phys. 46 (3), 329–340. https://doi.org/10.1016/0021-9991(82)
- Mahjoub, M., Dao, N.H., Summersgill, M., Menand, S., 2023. Fluid circulation effects on torque and drag results, modeling, and validation. SPE Drill. Complet. 1–12. https://doi.org/10.2118/212558-PA.
- Martins, A.L., Santana, M.L., Campos, W., Gaspari, E.F., 1999. Evaluating the transport of solids generated by shale instabilities in ERW drilling. SPE Drill. Complet. 14 (4), 254–259. https://doi.org/10.2118/59729-PA.
- Miao, H., Qiu, Z., Dokhani, V., Ma, Y., Zhang, D., 2023. Numerical modeling of transient cuttings transport in deviated wellbores. Geoen 211875. https:// doi.org/10.1016/j.geoen.2023.211875.
- Mitchell, R., Samuel, R., 2009. How good is the torque/drag model? SPE Drill. Complet. 24 (1), 62–71. https://doi.org/10.2118/105068-PA.
- Naganawa, S., Nomura, T., 2006. Simulating transient behavior of cuttings transport over whole trajectory of extended-reach well. The IADC/SPE Asia Pacific Drilling Technology Conference and Exhibition, Bangkok, Thailand. https://doi.org/ 10.2118/103923-MS
- Naganawa, S., Sato, R., Ishikawa, M., 2017. Cuttings-transport simulation combined with large-scale-flow-loop experimental results and logging-while-drilling data for hole-cleaning evaluation in directional drilling. SPE Drill. Complet. 32 (3), 194–207. https://doi.org/10.2118/171740-PA.
- Nguyen, D., Rahman, S.S., 1998. A three-layer hydraulic program for effective cuttings transport and hole cleaning in highly deviated and horizontal wells. SPE Drill. Complet. 13 (3), 182–189. https://doi.org/10.2118/51186-PA.
- Oroskar, A.R., Turian, R.M., 1980. The critical velocity in pipeline flow of slurries. AIChE J. 26 (4), 550–558. https://doi.org/10.1002/aic.690260405.
- Ramadan, A., Skalle, P., Saasen, A., 2005. Application of a three-layer modeling approach for solids transport in horizontal and inclined channels. Chem. Eng. Sci. 60 (10), 2557–2570. https://doi.org/10.1016/j.ces.2004.12.011.
- Shi, X., Huang, W., Gao, D., 2023a. Mechanical models of drillstrings with drag reduction oscillators and optimal design methods of vibration parameters in horizontal drilling. Geoen 224, 211585. https://doi.org/10.1016/j.geoen.2023.211585.
- Shi, X.L., Huang, W.J., Gao, D., Zhu, N., Li, W., 2023b. Extension limit analysis of drillstring with drag reduction oscillators in horizontal drilling. Geoen 211996. https://doi.org/10.1016/j.geoen.2023.211996.
- Sifferman, T.R., Becker, T.E., 1992. Hole cleaning in full-scale inclined wellbores. SPE Drill. Eng. 7 (2), 115–120. https://doi.org/10.2118/20422-PA.

- Song, X.Z., Pang, Z., Xu, Z.M., Li, G., Sun, B., Zhu, Z., Lyu, Z., 2019. Experimental study on the sliding friction for coiled tubing and high-pressure hose in a cuttings bed during microhole-horizontal-well drilling. SPE J. 24 (5), 2010–2019. https:// doi.org/10.2118/194192-PA.
- Tong, T.A., Ozbayoglu, E., Liu, Y., 2021. A transient solids transport model for solids removal evaluation in coiled-tubing drilling. SPE J. 26 (5), 2498–2515. https:// doi.org/10.2118/205370-PA.
- Walton, I.C., 1995. Computer simulator of coiled tubing wellbore cleanouts in deviated wells recommends optimum pump rate and fluid viscosity. SPE Production Operations Symposium, Oklahoma City, USA. https://doi.org/10.2118/ 29491-MS.
- Wang, Z., 2008. Fluid Mechanics in Petroleum Engineering. Petroleum industry press, Beijing.
- Zhang, F.F., Miska, S., Yu, M., Ozbayoglu, E., 2018. A unified transient solid-liquid two-phase flow model for cuttings transport-modelling part. J. Petrol. Sci. Eng. 166, 146–156. https://doi.org/10.1016/j.petrol.2018.03.027.
- Zhang, F.F., Islam, A., Zeng, H., Chen, Z., Zeng, Y., Wang, X., Li, S., 2019. Real time stuck pipe prediction by using a combination of physics-based model and data analytics approach. The Abu Dhabi International Petroleum Exhibition & Conference, Abu Dhabi, UAE. https://doi.org/10.2118/197167-MS.
- Zhang, F.F., Wang, Y., Wang, Y., Miska, S., Yu, M., 2020. Modeling of dynamic cuttings transportation during drilling of oil and gas wells by combining 2D CFD and 1D discretization approach. SPE J. 25 (3), 1220–1240. https://doi.org/10.2118/1990.2-PA
- Zhao, J., Huang, W.J., Gao, D.L., Zhao, L., 2022a. Mechanism analysis of the regular

- pipe sticking in extended-reach drilling in the eastern South China Sea. The 56th U.S. Rock Mechanics/Geomechanics Symposium Santa Fe, New Mexico, USA. https://doi.org/10.56952/ARMA-2022-0563.
- Zhao, J., Huang, W.J., Gao, D.L., 2022b. Research on dynamic prediction of tubular extension limit and operation risk in extended-reach drilling. J. Nat. Gas Sci. Eng. 107, 104542. https://doi.org/10.1016/j.jngse.2022.104542.
- Zhao, J., Huang, W.J., Gao, D.L., 2024. Interaction between pipe rotation and cuttings transport in extended-reach drilling: mechanism, model, and applications. SPE J. 29 (6), 2857–2876. https://doi.org/10.2118/219483-PA.
- Zhu, N., 2022. Study on Cuttings Transport and Pipe Stuck Mechanism in Extended-Reach Drilling. PhD Dissertation. China University of Petroleum, Beijing.
- Zhu, N., Huang, W.J., Gao, D.L., 2021. Dynamic wavy distribution of cuttings bed in extended reach drilling. J. Petrol. Sci. Eng. 198, 108171. https://doi.org/10.1016/ i.petrol.2020.108171.
- Zhu, N., Huang, W.J., Gao, D.L., 2022. Numerical analysis of the stuck pipe mechanism related to the cutting bed under various drilling operations. J. Petrol. Sci. Eng. 208, 109783. https://doi.org/10.1016/j.petrol.2021.109783.
- Zhu, N., Ding, S.D., Shi, X.L., Huang, W., Gao, D., 2023. Numerical analysis of the connector effect on cuttings bed transportation while Tripping. Geoen 227, 211817. https://doi.org/10.1016/j.geoen.2023.211817.
- Zhu, X., Wang, X., Liu, Y., Luo, Y., Zhang, H., 2024. Probing the effect of cuttings particle size on the friction and wear mechanism at the casing friction interface: a molecular dynamics study. J. Mol. Liq. 396, 124006. https://doi.org/10.1016/j.molliq.2024.124006.